

The Dynamic Response
of
A Laminar Flow Heat Exchanger

By
Hyung K. Zang

ProQuest Number: 10795870

All rights reserved

INFORMATION TO ALL USERS

The quality of this reproduction is dependent upon the quality of the copy submitted.

In the unlikely event that the author did not send a complete manuscript and there are missing pages, these will be noted. Also, if material had to be removed, a note will indicate the deletion.



ProQuest 10795870

Published by ProQuest LLC (2018). Copyright of the Dissertation is held by the Author.

All rights reserved.

This work is protected against unauthorized copying under Title 17, United States Code
Microform Edition © ProQuest LLC.

ProQuest LLC.
789 East Eisenhower Parkway
P.O. Box 1346
Ann Arbor, MI 48106 – 1346

A Thesis submitted to the Faculty and the Board of Trustees of the Colorado School of Mines in partial fulfillment of the requirements for the degree of Doctor of Science.

Signed: Hyunghoon Zang

Golden, Colorado

Date: Sept. 12, 1967

Approved: Franklin Stemple
Thesis Advisor

James H. Gary
Head of Department

Golden, Colorado

Date: Sept. 12, 1967

ABSTRACT

This study consisted of two basic factors: (1) a theoretical investigation of the dynamic response of a laminar flow heat exchanger subjected to disturbances of flow rate, inlet temperature, wall temperature, and wall heat-flux, and (2) an experimental investigation of the dynamic response of a laminar-flow heat exchanger subjected to step upsets in flow rate with uniform wall heat flux. Theoretical and experimental dynamic response data were compared.

Partial differential equation models which took into account axial convection and radial conduction of energy were solved for various combinations of disturbances of flow rate, inlet temperature, wall temperature, and wall heat-flux. Step and sinusoidal disturbances were considered for these variables as a function of time and as a function of axial distance for wall temperature and wall heat-flux.

The dynamic temperature response of heat exchanger fluid

subjected to step upsets in fluid flow rate with uniform wall heat-flux was selected for the experimental investigation. A 5-ft heat exchanger was constructed with a 1/2-in. copper tube whose outside wall was heated by wound electrical resistance wire. A mixture of glycerine and water (59%, 43%, and 0% glycerine by volume) was passed through the heat exchanger tube. Dynamic fluid temperature response was observed at different radial positions for step increases and decreases in fluid-flow rate. Fluid-flow rates varied from Reynolds numbers of 70 to 3875.

TABLE OF CONTENTS

	Page
LIST OF FIGURES.	vii
LIST OF TABLES	x
ACKNOWLEDGMENT	xi
INTRODUCTION AND LITERATURE SURVEY	1
EXPERIMENTAL INVESTIGATION	8
Apparatus	12
Liquid Circulating System.	12
Heat Exchanger	14
Temperature Measuring System	16
Procedure	17
Results	20
THEORETICAL INVESTIGATION.	22
DISCUSSION OF EXPERIMENTAL AND THEORETICAL RESULTS . .	54
CONCLUSIONS.	95
LITERATURE CITED	99
NOMENCLATURE	102

	Page
APPENDIX	
A Steady-state Data for the Ten Experimental Runs	105
B Steady-state Theoretical Data for a Step Change in Inlet Temperature	110
C Steady-state Theoretical Data for a Step Change in Flow Rate	111
D Physical Properties of the Liquids	112

LIST OF FIGURES

Figure	Page
1. Distribution of velocity profile due to variable viscosity	6
2. Flow diagram of experimental apparatus	11
3. Experimental and theoretical fluid temperature response to transient flow changes between 0.273 ft/sec and 0.467 ft/sec with uniform wall heat-flux	62
4. Experimental and theoretical fluid temperature response to transient flow changes between 0.188 ft/sec and 0.309 ft/sec with uniform wall heat-flux	64
5. Experimental and theoretical fluid temperature response to transient flow changes between 0.188 ft/sec and 0.42 ft/sec with uniform wall heat-flux	66

Figure	Page
6. Experimental and theoretical fluid temperature response to transient flow changes between 0.228 ft/sec and 0.448 ft/sec with uniform wall heat-flux	68
7. Experimental and theoretical fluid temperature response to transient flow changes between 0.228 ft/sec and 0.337 ft/sec with uniform wall heat-flux	70
8. Experimental and theoretical fluid temperature response to transient flow changes between 0.289 ft/sec and 0.438 ft/sec with uniform wall heat-flux	72
9. Experimental and theoretical fluid temperature response to transient flow changes between 0.269 ft/sec and 0.568 ft/sec with uniform wall heat-flux	74
10. Experimental and theoretical fluid temperature response to transient flow changes between 0.269 ft/sec and 0.371 ft/sec with uniform wall heat-flux	76
11. Experimental and theoretical fluid temperature response to transient flow changes between 0.269 ft/sec and 0.682 ft/sec with uniform wall heat-flux	78

Figure	Page
12. Experimental and theoretical fluid temperature response to transient flow changes between 0.269 ft/sec and 0.353 ft/sec with uniform wall heat-flux	80
13. Experimental and theoretical fluid temperature vs radial position for Run 7 with time as a parameter.	85
14. Theoretical fluid temperature response to transient inlet temperature changes between 70°F and 105°F with uniform wall temperature . .	89
15. Theoretical fluid temperature response to transient flow changes between 0.269 ft/sec and 0.685 ft/sec with uniform wall temperature .	92
16. Qualitative change in velocity profile by natural convection proposed by Oliver.	94

LIST OF TABLES

Table	Page
1. The range of N_{Gr}/N_{Re}^2 in determining the predominant effect of natural or forced convection	59
2. Initial and final steady-state data for ten experimental runs.	105
3. Initial and final steady-state theoretical data for a step change in inlet temperature with uniform wall temperature.	110
4. Initial and final steady-state theoretical data for a step change in flow rate with uniform wall temperature	111
5. Physical properties of glycerine-water mixtures at 30°C	112
6. Experimental transient data for ten experimental runs.	113

ACKNOWLEDGMENT

The author wishes to express his appreciation to Dr. Franklin J. Stermole for his inspiring guidance, valuable advice, and suggestions through this research project.

The author is also grateful to Dr. James Gary, Chairman of the Department, who frequently gave help during the author's investigations.

The financial support provided by the Colorado School of Mines Foundation was greatly appreciated.

INTRODUCTION AND LITERATURE SURVEY

In recent years, the dynamic behavior of heat exchangers has increased in importance with the advent of faster and more sensitive closed loop control of heat exchanger systems. Publications which pertain to unsteady-state heat transfer in a tube, duct, or channel have been increased greatly. A considerable amount of work has been done on turbulent-flow unsteady-state heat transfer in a tube. Many investigators have studied this problem of heat exchanger dynamics in which the radial conduction is negligible because of perfect radial mixing of fluid under turbulent flow conditions.

It is clear from theoretical considerations that the dynamic behavior of a heat exchanger for laminar flow and turbulent flow cannot be explained in the same way if radial temperature variation is considered since the heat transfer mechanisms are different. In turbulent flow the temperature profile in a tube is almost flat in the turbulent core, but

the temperature profile in the laminar sublayer, where radial conduction plays a significant role, is very steep. In laminar flow, since the temperature profile in a tube is very much dependent on the radial position across the tube, radial conduction cannot be neglected.

Because of the difficulty of solving the appropriate differential equations when the contribution of radial conduction is significant, very little previous work that accounts for radial conduction has been reported for heat exchanger dynamics. As precise control of systems is required in modern technology applications, accurate mathematical descriptions of these systems and the solutions of the corresponding mathematical models with fewer assumptions are needed.

Sparrow⁽¹⁾, Siegel⁽²⁾, and Perlmutter⁽³⁾ either independently or with coworkers, have investigated various problems of unsteady-state heat transfer in both laminar- and turbulent-flow regimes where radial conduction was taken into account.

Siegel⁽⁴⁾ solved the problem of unsteady-state laminar-flow heat transfer in ducts using the approximation that the isothermal Hagen-Poiseuille velocity profile was valid for non-isothermal conditions. Approximation solutions were given which were obtained from the integrated energy

equation rather than from the differential energy equation. Solutions were obtained for the limiting cases of small and large time. These limiting solutions were in turn used to construct an approximate result applicable for all values of time. No experimental verification of this model was given.

By using a multiple transform method, Chu and Bankoff⁽⁵⁾ solved three cases of unsteady-state heat transfer for plug-flow conditions, while taking axial conduction into account for wall-temperature upsets to a semi-infinite tube, semi-infinite parallel plates, and infinite parallel plates. In all three cases only tube-fluid temperature was dependent on spatial and time variables, and the fluid velocity remained constant. Plots were presented for axial distance versus mean temperature of a semi-infinite plate, mean temperature difference, and mean Nusselt number difference between cases of infinite and semi-infinite parallel plates. Comparisons were made with and without axial conduction for various Peclet numbers and times. No attempt was made to obtain temperature profiles with velocity changes.

Siegel and Perlmutter⁽³⁾ solved the problem of unsteady-state laminar-flow heat transfer in a rectangular channel with wall flux as a function of time and axial position. Only limited cases were presented for wall-flux changes by assuming that the channel and fluid were isothermal in steady

state. The solutions were first obtained in Lagrangian coordinates and then transformed back to Eulerian coordinates. One form of heat flux change utilized was $q/q_s = (1 - e^{-Ax^*})(1 - e^{-Bt^*})$, where A and B are constants.

Zeiberg and Mueller⁽⁶⁾ investigated transient, free, and forced laminar convection in a duct. Solutions of momentum and energy equation were obtained by Green's function technique with the uncoupling of two equations. Several extreme cases of free and forced laminar convection were presented.

The two prime purposes of this investigation of laminar flow heat exchanger dynamics are (1) the development of a mathematical model for predicting the dynamic response of a tubular heat exchanger subjected to various forcing functions and (2) an experimental investigation of tubular heat exchanger dynamics for step upsets in flow rate. Experimental results and the corresponding mathematical model are compared. Theoretical solutions are obtained for various forcing functions by applying Hankel transform techniques and the characteristic method to the unsteady-state partial differential equation which accounts for axial bulk flow and radial conduction of heat with average fluid velocity. Step and sinusoidal forcing functions, which are useful in theoretical and experimental aspects of process control, are

considered.

The experimental system selected for this study is a circular tube with a thin wall of negligible capacitance. A steady state temperature profile which is a function of radial and axial position exists within the tube fluid before the onset of forcing functions. At the entrance of the tube the temperature distribution within the fluid is uniformly constant. At time zero, a known forcing function is applied and the fluid temperature response is observed at the exchanger outlet at various radial positions.

In an isothermal system the steady-state laminar-flow velocity profile in a tube obeys the Hagen-Poiseuille equation. In a non-isothermal system, such as the one studied here, because physical properties of the system vary with temperature, the velocity profile would not necessarily agree with the Hagen-Poiseuille equation. In general, it is uncertain in non-isothermal laminar-flow heat-transfer systems how the velocity of the fluid varies exactly with respect to the spatial dimensions. It is shown in Fig. 1 by McAdams⁽⁷⁾ how variation of viscosity with respect to temperature affects the velocity distribution in a tube. If the variation of density, which causes natural convection, is taken into account in addition to the variation of viscosity, the distorted velocity profile of heated liquid

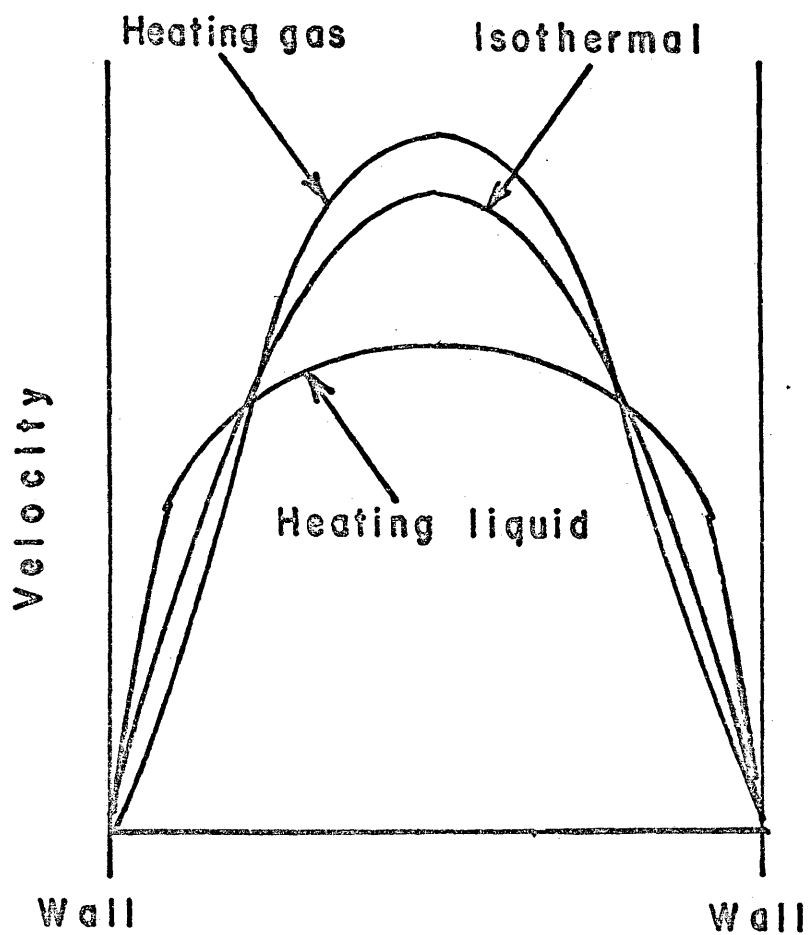


Fig.1. Distribution of velocity profile due to variable viscosity

would be somewhat more rodlike and the temperature profile would be very flat in the central region of the tube.

In practice, it is very common to use mean values of physical properties and fluid velocity. It has been found by Kirkbride and McCabe⁽⁸⁾ that when variations of physical properties due to non-isothermal conditions cannot be accounted for theoretically, especially for the heating of liquid in a tube, the solution for the flat velocity profile in the laminar flow agrees better with experimental data than with the solution for the parabolic Hagen-Poiseuille velocity profile. This discrepancy has been explained by Kirkbride and McCabe on the basis of change in the physical properties.

An exact solution of this heat exchanger problem which takes into account all the variations of physical properties and the velocity profile in accordance with the appropriate physical laws is beyond the reach of present mathematical techniques due to the complexity of resulting equations to be solved. Simplifications are necessary to obtain a solution for this problem. On the basis of the previous work cited in this thesis, it is felt that the assumptions utilized in this study yield a valid approach to this heat transfer dynamics problem.

EXPERIMENTAL INVESTIGATION

Many chemical processes are controlled automatically today. Temperature, pressure, and concentration can be controlled closely by very modern control systems. Of the many ways of controlling a process, one of the popular means is regulating a flow rate. Variation of flow rate in a chemical process often is inherent or desirable from a control point of view. Many specific applications may be cited. Variation of the coolant flow rate often is used to control the reaction temperature in a reactor. Variation of flow rates of feed and recycle streams of a distillation column changes the concentration of the top and bottom products. Changing fluid flow rate through a heat exchanger can be used to control the outlet fluid temperature. Since process-flow-rate dynamics plays a major part in chemical systems control, this experimental investigation was focused on flow rate upsets to a laminar-flow heat exchanger with uniform wall-flux.

A schematic diagram of experimental equipment for measuring the transient temperature profile for flow-rate upsets within a vertical tube is shown in Fig. 2. A glycerine-water mixture and pure water were used for the fluid media. These fluids were pumped from the feed tank to the constant head tank which was mounted in an elevated position eleven feet above the outlet of the heat exchanger. Glycerine-water mixture or water was then introduced to the inlet of the calming section of the heat exchanger by the gravitational force and passed through the exchanger, where it was heated by wound electrical resistance wire. After leaving the heat exchanger, the liquid was cooled in a secondary counter current heat exchanger and then passed on to the reservoir tank.

The transient radial temperature response of the liquid was measured five feet above the inlet of the test section of the heat exchanger with a 1/16-in. OD iron-constantin thermocouple introduced from the wall of the heat exchanger. Signals from the thermocouple were recorded on a single-channel strip-chart recorder.

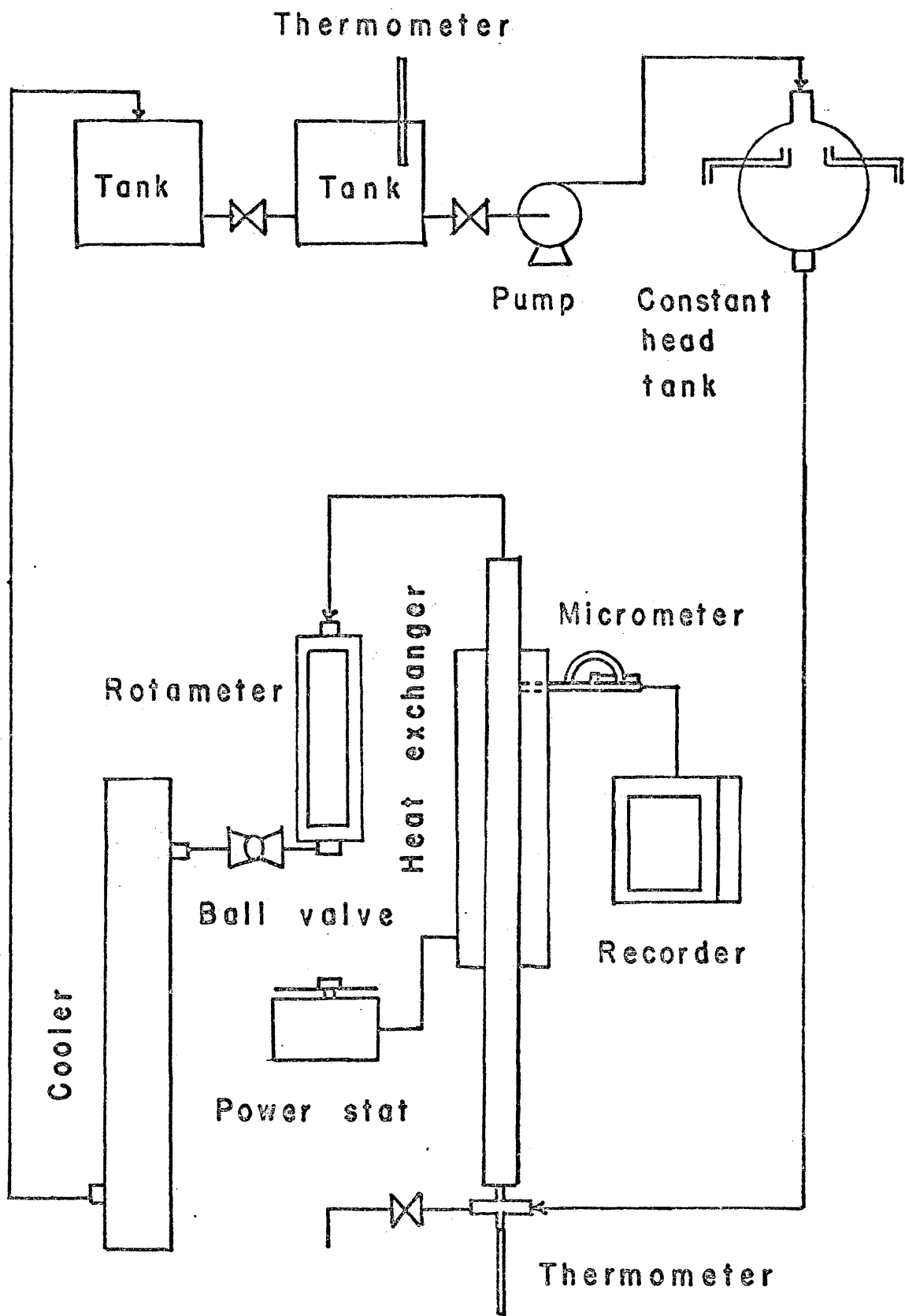
The experimental investigation will be discussed under the following three headings:

Apparatus

Procedure

Results

Figure 2. Flow diagram of experimental apparatus.



Apparatus

The apparatus consisted of a pump, constant liquid head tank, feed line, test heat exchanger, temperature measuring device, flow control valve, rotameter, cooling counter current exchanger, and two feed tanks.

Liquid Circulating System: Three liquids were used in this study: (1) pure water; (2) 59% glycerine, 41% water; and (3) 43% glycerine, 57% water by volume. The present experimental work was directed toward a correlation of experimental and theoretical transient temperature profiles for laminar-flow flow-rate upsets. Therefore, it was deemed advisable to choose fluid flow rates with as wide a range of Reynolds number as possible up to transition region. Many liquids would give the desired physical properties. However, the glycerine-water system was chosen because glycerine mixes well with water, and the physical properties of glycerine-water mixtures do not change drastically with respect to temperature. Also, a wide range of fluid viscosity can be obtained by varying glycerine-water ratio. Pure water, which has lower viscosity than the glycerine-water mixture, was chosen to run experiments at high Reynolds number. The glycerine used in this study was chemically pure to specifications of U. S. pharmacopoeia.

For the elimination of flow disturbances introduced by

direct pumping of fluid, a constant head tank was built and gravitational force was used to force liquid through the system.

Liquid was pumped from a ten-gallon stainless-steel tank to the constant head tank by a 1/3-hp centrifugal pump. The constant head tank was constructed of a standard 2000-ml pyrex-glass flask mounted in an elevated position eleven feet above the heat exchanger outlet. It had two overflow outlets in its side and the bottom was connected to the feed line by a 3/8-in. hole. Overflow from the constant head tank was returned to the feed tank, which step helped the mixing of liquid in the tank. Liquid was introduced to the inlet of the calming section of the heat exchanger by gravitational force and passed through the test and cooling heat exchangers. After leaving the exchangers, the liquid was stored in another ten-gallon stainless-steel tank for later experimental runs. Since it was necessary to know the rate of flow through the heat exchanger very accurately, a rotameter (Fischer-Porter FP-1/2-27-G-10/83) for measuring liquid-flow rate was installed between the ball valve and the cooling heat exchanger. Flow of liquid through the heat exchanger was regulated manually by a 1/4-in. Jenkins ball valve. With this type of valve it was possible to produce a rapid change in flow without any lag. Because the fluid was incompressible,

location of the valve did not affect the flow-rate control.

For the control of the opening of the valve, a bar with stops on it was installed parallel to the direction of flow so that the valve handle moved across the bar. With this arrangement, it was possible to set the stops on the bar so that when the handle of the valve was quickly moved between them, a step change of known flow rate was obtained. Flow rates were calibrated for these stops before each run and, of course, the high and low rates of flow were observed on the rotameter.

Heat Exchanger: The test heat exchanger was made with a 1/2-in. nominal diameter, type-L copper tube, 8-feet in length and mounted vertically. It had an inside diameter of 0.585-in. and wall thickness of 0.05-in. An entrance length of 2 ft for a calming section was extended from the inlet of the test section to eliminate turbulence and establish a fully developed laminar-flow velocity profile. The entrance length used for laminar flow is given by Bird, Stewart, and Lightfoot⁽⁹⁾ as

$$L_e = 0.035 \times D \times N_{Re}$$

where N_{Re} is the Reynolds number of the fluid and D is the diameter of the tube. For the present experimental study,

L_e was about 1.7 ft for a Reynolds number of 2000 (the upper limit of laminar flow). At the exchanger exit, the last 1 ft of the heat exchanger tube served as the exit velocity-calming section in order not to disturb the flow at the point of the temperature measurement, which was the end of the 5 ft heat exchanger length.

Copper tube was chosen for the heat exchanger, because of its high thermal conductivity and its availability with very thin walls. These walls make thermal capacitance of the wall essentially negligible.

Uniform heat flux was obtained by heating the liquid with uniform dissipation of electrical energy supplied by the wound electrical resistance wire (B&S 20 Nichrome wire), which was wound every 0.15 in. of the axial distance of the heat exchanger. A thin layer of asbestos paper estimated to be 0.029 in. thick was used as the electrical insulator between the wall of the heat exchanger and the heating element. This layer of asbestos paper gave adequate electrical insulation with satisfactory thermal conductivity. On top of the electrical heating element a 0.06-in. layer of asbestos paper and $1\frac{1}{2}$ -in. of 85% magnesia thermal insulation were installed.

A calibrated clamp-on ammeter and volt meter were attached to a power stat to control and measure the power

input to the heating element. The power input to the heating element was regulated by two 2-KVA power stats connected in parallel.

Temperature Measuring System: Transient radial temperature profiles of liquids at 5 ft above the inlet of the test section were measured with a 1/16-in. OD jacketed iron-constantin thermocouple. The response time constant of the thermocouple was two-tenths of a sec for step changes in liquid temperature. In the installation of the thermocouple a 1/8-in. adjustable bushing was welded to the wall of the heat exchanger and a 1/16-in. diameter hole was drilled through the center of the bushing and the wall of the heat exchanger. Through this hole the thermocouple was inserted. The adjustable bushing with a nylon internal sleeve made it possible to vary the immersion length of the thermocouple, which in turn made it possible to take various radial readings of temperatures.

Radial distances in the heat exchanger tube where temperatures were read were measured by a micrometer mounted parallel to the path of the thermocouple. The micrometer used in the study was graduated from zero to one inch in 0.001-in. increments. A holder was made from a rubber tubing clamp with thumb screw attached to the thermocouple lead. The distance the holder moved was measured by a

micrometer. The reading of the radial distance was reproduced within 0.01-in.

Fluid temperature was monitored at different radial positions with a strip-chart recorder to obtain the desired dynamic response data. Millivolt signals from the thermocouple were recorded on a Mozley model 680 single-channel recorder with 1 millivolt full-scale sensitivity. The thermocouple and recorder were calibrated by using a constant temperature bath. Temperature readings were reproducible during the calibration, and it was determined that the temperature measuring system was satisfactory for the present study.

Bulb thermometers with mercury-in-glass were placed at the inlet of the heat exchanger, at the outlet of the cooling exchanger, and in the feed tank to measure any existing temperature difference between the feed tank and the inlet of the heat exchanger.

Procedure

To start an experimental run, the switch for the pump was turned on, and the glycerine-water mixture was pumped from the feed tank to the constant head tank. Liquid was passed through the system by gravitational force. The flow rate at this moment was regulated by the gate valve

positioned between the feed tank and constant head tank. An overflow was always maintained in the constant head tank. The ball valve at this time was fully open. The power input to the heating element was applied and regulated to give the appropriate heat flux.

Next, the thermocouple terminal was connected to the recorder. The thermocouple and recorder were calibrated before experimental runs. The ball valve openings were adjusted to set two stops on the bar for high and low rates of flow. A quick move of the valve handle between these two positioned stops produced the desired step change in liquid flow rate. Liquid flow rates were read with a rotameter at high and low flow rates. The gate valve was then adjusted, if necessary, to maintain overflow from the constant head tank.

The system was then allowed to come to a steady state at the low flow rate. Steady state temperatures at various radial positions were checked. Positions to measure transient temperature were determined as follows: (1) the radial position was found where the temperature was lowest; (2) With the aid of the recorder, the difference between the millivolt signal from the wall of the heat exchanger and the point of lowest temperature was divided by three. These three millivolt signals were noted on the strip-chart of the

recorder. Three radial positions on the other wall side were determined in the same way. The order of measuring radial transient temperatures was from the wall to the center (position at lowest temperature) and then to the other wall. In general, transient temperatures at seven radial positions were observed. However, it was found that radial temperatures measured near the wall from which the thermocouple protruded were in significant error due to thermal conduction along the thermocouple from the hot wall. Calculations to determine measured temperature error due to thermal conduction indicated that the errors were much smaller from the center line to the opposite wall, so that most experimental data were taken in these locations.

When the temperature reading on the recorder showed that the temperature at a radial position had reached a constant value, the step increase in flow rate was made by quickly opening the valve. After the transient response was completed and a new steady state was achieved, the valve handle was moved quickly to its lower position to produce the step decrease in flow rate. The same step changes were repeated for each radial temperature measurement.

Transient-temperature response curves for step changes in flow rate were recorded for various upset magnitudes with three different wall heat fluxes. Each run was repeated

three times or more to assure that data were reproducible.

Care was exercised to prevent any air trap in the system, when a run was started by partially draining the liquid from the bottom of the heat exchanger. Whenever the presence of the rust was noted, the whole apparatus was cleaned carefully. Before every run, the inlet temperature was observed and recorded.

Results

Ten experimental tests were conducted over various magnitudes of step upsets in liquid flow rate at three different wall heat fluxes. Steady-state data for the maximum and minimum flow rates of the ten runs are presented in Table 2. Transient temperature profiles at the heat exchanger exit were obtained for increases and decreases in liquid flow rate between these levels. Transient response data for increases and decreases in liquid flow rate are presented in Figs. 3 through 12, and in Table 6.

The step upsets represented both small and large departures from the initial steady-state values. Flow increases and decreases of magnitudes that were from 39 to 155 percent of the initial steady-state value were conducted for wall heat fluxes of 817, 1115, and 1900 Btu/hr.ft². The range of N_{Re} was from 70 to 3875.

Physical properties of the liquids were taken from the International Critical Tables⁽¹⁰⁾ with the exception of the densities of the liquids which were measured experimentally. They are presented in Table 5.

THEORETICAL INVESTIGATION

Several investigators have previously studied unsteady state laminar-flow heat transfer in a tube, duct, or channel, but most of them have been for either wall temperature or wall heat-flux change only. Less attention has been given to the problem of unsteady-state laminar-flow heat transfer with change of flow rate or combinations of change of flow rate, inlet temperature, wall temperature, and wall heat flux due to the complexity of the problem.

In the present work, theoretical solutions are obtained by applying Hankel transform techniques and the characteristic method to the unsteady-state partial differential equation which accounts for axial bulk flow and radial conduction of heat with average fluid velocity. A steady-state temperature profile which is a function of radial and axial position exists within the fluid before the onset of forcing functions to the flow rate, inlet temperature, wall temperature, and wall heat-flux; At the entrance of the tube the temperature

distribution is considered to be uniform across the tube and designated as T_1 .

At time zero, known forcing functions are applied and fluid temperature response is predicted. Time variable forcing functions are considered first and then position variable forcing functions are considered.

Mathematical Analysis

A mathematical description of a tubular heat exchanger with axial convection and radial conduction is obtained by writing an energy balance over a differential fluid element.

$$\frac{\partial T}{\partial t^*} + u \frac{\partial T}{\partial x^*} = \frac{k}{r^*} \frac{\partial}{\partial r^*} \left(r^* \frac{\partial T}{\partial r^*} \right) \quad (1)$$

The assumptions made in deriving equation (1) are:

1. The fluid is incompressible
2. Axial heat conduction and viscous dissipation are negligible
3. The variation of fluid properties with temperature is negligible
4. Natural convection is negligible

Starting with equation (1), several mathematical models have been developed to relate fluid temperature to various

upsets. Upsets of flow rate, inlet temperature, wall temperature, and wall heat-flux have been considered.

First, consider the dynamic response models for upsets of flow rate, inlet temperature, and wall temperature.

Equation (1) describes the system, and the boundary conditions to be satisfied are:

$$\begin{aligned}
 1. \quad t^* = 0, \quad T &= T_s \\
 2. \quad x^* = 0, \quad T &= T_i \\
 3. \quad r^* = 0, \quad \frac{\partial T}{\partial r^*} &= 0 \\
 4. \quad r^* = R, \quad T &= T_w
 \end{aligned} \tag{2}$$

Now define new dimensionless variables as follows:

$$\theta = \frac{T}{T_w}, \quad r = \frac{r^*}{R}, \quad x = \frac{4x^*}{DN_{Res} N_{pr}}, \quad t = \frac{4u_s t^*}{DN_{Res} N_{pr}} \tag{2a}$$

In terms of these new variables equation (1) becomes

$$\frac{\partial \theta}{\partial t} + \{1 + a(t)\} \frac{\partial \theta}{\partial x} = \frac{1}{r} \frac{\partial}{\partial r} \left(r \frac{\partial \theta}{\partial r} \right) \tag{3}$$

where

$$a(t) = u'(t)/u_s \tag{4}$$

In terms of the new variables boundary conditions which must be satisfied are:

1. $t = 0, \quad \theta = \theta_s$
2. $x = 0, \quad \theta = b(t)$ (4)
3. $r = 0, \quad \frac{\partial \theta}{\partial r} = 0$
4. $r = 1, \quad \theta = c(t)$

where, $b(t) = T_i(t)/T_{ws}$ (5)

$$c(t) = T_w(t)/T_{ws} \quad (6)$$

Define the Hankel transform

$$\bar{\theta} = \int_0^1 \theta r J_0(\alpha_n r) dr \quad (7)$$

where α_n is a root of

$$J_0(\alpha_n) = 0 \quad (8)$$

where n is taken over all the possible zeroes of equation (8).

Multiplying both sides of equation (3) by $rJ_0(\alpha_n r)$ and

integrating with respect to r from 0 to 1,

$$\int_0^1 \frac{\partial \theta}{\partial t} r J_0(\alpha_n r) dr + \int_0^1 \{1+a(t)\} \frac{\partial \theta}{\partial x} r J_0(\alpha_n r) dr =$$

$$\int_0^1 \frac{\partial}{\partial x} \left(r \frac{\partial \theta}{\partial r} \right) J_0(\alpha_n r) dr \quad (9)$$

Integrating the right side of equation (9) by parts gives

$$\frac{\partial \bar{\theta}}{\partial t} + \{1 + a(t)\} \frac{\partial \bar{\theta}}{\partial x} + \alpha_n^2 \bar{\theta} = \alpha_n J_1(\alpha_n) C(t) \quad (10)$$

Equations (4), (7), and (8) are used to obtain equation (10). Equation (10) may be solved by the method of characteristics as presented by Sneddon⁽¹¹⁾. According to this method, equation (10) is rewritten as two ordinary differential equations:

$$dt = \frac{dx}{1+a(t)} = \frac{-d\bar{\theta}}{\alpha_n^2 \bar{\theta} - \alpha_n J_1(\alpha_n) C(t)} \quad (11)$$

Equating the first and second members of equation (11) and solving

$$t + \int_0^t a(\tau) d\tau - x = C_1 \quad (12)$$

Similarly, using the first and third members,

$$\frac{1}{\alpha_n^2} \ln \{ \alpha_n^2 \bar{\theta} - \alpha_n J_1(\alpha_n) C(t) \} + t = C_2 \quad (13)$$

Here C_1 and C_2 are arbitrary constants. The general solution to equation (10) is obtained by putting $C_2 = f(C_1)$, where f is an arbitrary function. Thus:

$$\frac{1}{\alpha_n} \ln \left\{ \alpha_n^2 \frac{2}{\theta} - \alpha_n J_1(\alpha_n) C(t) \right\} + t =$$

(14)

$$f \left\{ t + \int_0^t a(\tau) d\tau - x \right\}$$

When $x = 0$, equation (14) becomes

$$\frac{1}{\alpha_n} \ln \left\{ b(t) \alpha_n J_1(\alpha_n) - C(t) \alpha_n J_1(\alpha_n) \right\} + t =$$

(15)

$$f \left\{ t + \int_0^t a(\tau) d\tau \right\}$$

This is a functional relationship for an unknown function f .

Let

$$y = t + \int_0^t a(\tau) d\tau$$

(16)

Then

$$t = y - \int_0^{g(y)} a(\tau) d\tau$$

(17)

where $g(y)$ is a function satisfying

$$g(y) = y - \int_0^{g(y)} a(\tau) d\tau \quad (18)$$

Substitute equations (16) and (17) into equation (15) and obtain

$$f(y) = y - \int_0^{g(y)} a(\tau) d\tau + \frac{1}{\alpha_n^2} \ln \{ \alpha_n J_1(\alpha_n) b(t) - C(t) \} \quad (19)$$

Now that the function f is known, it may be used in equation (14) to obtain the solution for $\bar{\theta}$.

$$\bar{\theta} = \frac{J_1(\alpha_n)}{\alpha_n} \{ b(t) - C(t) \} \exp \left\{ \alpha_n^2 \int_G^t a(\tau) d\tau - \alpha_n^2 x \right\} + \frac{J_1(\alpha_n)}{\alpha_n} C(t) \quad (20)$$

$$\text{where } G = g \left\{ t + \int_G^t a(\tau) d\tau - x \right\}$$

The function G may be eliminated from the solution by utilizing equation (18).

$$G = t + \int_G^t a(\tau) d\tau - x \quad (21)$$

Equation (20) is solved for step and sinusoidal forcing

functions to flow rate, inlet temperature, and wall temperature.

Case 1. Flow Rate Upsets with Uniform Wall Temperature

At $t = 0$, variations of fluid flow rate from the steady state are applied to the system and the temperature response of fluid is predicted.

Case 1a. Step Change in Flow Rate

$$\text{Let } a(t) = aU(t) \quad (22)$$

where "a" is the magnitude of the step change and $U(t)$ is the unit step function.

$$U(t) = \begin{cases} 1 & t > 0 \\ 0 & t < 0 \end{cases} \quad (23)$$

Substitute equation (22) into equation (20) and solve equation (20) for $\bar{\theta}$. For this case $c(t) = 1$ and $b(t) = b_s$, where $b_s = T_{is}/T_{ws}$. It is easier in this case to solve equation (20) after $g(y)$ is obtained from equation (18).

$$g(y) = y - ag(y) \quad \text{or}$$

$$g(y) = \frac{y}{1+a} \quad (24)$$

$$g(t + at - x) = t - \frac{x}{1+a} \quad (25)$$

The solution for $\bar{\theta}$ is:

$$\bar{\theta} = \frac{J_1(\alpha_n)}{\alpha_n} \left\{ (b_s - 1) e^{-\frac{\alpha_n^2 x}{1+a}} + 1 \right\} \quad (26)$$

$$\text{for } t > \frac{x}{1+a}$$

$$\bar{\theta} = \frac{J_1(\alpha_n)}{\alpha_n} \left\{ (b_s - 1) e^{-\alpha_n^2 (x-at)} + 1 \right\} \quad (27)$$

$$\text{for } t < \frac{x}{1+a}$$

By the well known theory of Fourier-Bessel series presented in Watson⁽¹¹⁾, if α_n is a root of equation (8) and if θ can be represented in the range $0 < r < 1$ by

$$\theta(x, r, t) = \sum_n C_n J_0(\alpha_n r) \quad (28)$$

then the coefficients C_n are given by

$$C_n = \frac{2}{J_1^2(\alpha_n)} \int_0^1 \theta r J_0(\alpha_n r) dr \quad (29)$$

$$= \frac{2\bar{\theta}}{J_1^2(\alpha_n)}$$

Therefore, inversion of the Hankel transformation gives,

$$\theta(x,r,t) = \sum_n 2 \frac{J_0(\alpha_n r)}{J_1^2(\alpha_n)} \bar{\theta} \quad (30)$$

Substituting equations (26) and (27) into equation (30) gives the analytical solution for θ .

$$\theta = 2 \sum_n \frac{J_0(\alpha_n r)}{\alpha_n J_1(\alpha_n)} \left\{ (b_s - 1) e^{-\frac{\alpha_n^2 x}{1+a}} + 1 \right\} \text{ for } t > \frac{x}{1+a} \quad (31)$$

$$\theta = 2 \sum_n \frac{J_0(\alpha_n r)}{\alpha_n J_1(\alpha_n)} \left\{ (b_s - 1) e^{-\alpha_n^2 (x-at)} + 1 \right\} \text{ for } t < \frac{x}{1+a} \quad (32)$$

Case 1b. Sinusoidal Change in Flow Rate

$$a(t) = A \cos wt \quad (33)$$

where "A" is amplitude and "w" is the angular frequency in radians. Substitute equation (33) into equation (18) and obtain $g(y)$.

$$g(y) = y - \frac{A}{w} \sin \{wg(y)\} \quad (34)$$

Unfortunately, the response to a sinusoidal disturbance cannot be calculated explicitly by this method except in the secondary time domain, which is of secondary interest in the

sinusoidal response. The basic difficulty is the solution of equation (34) for $g(y)$, where equation (34) is implicit in $g(y)$. Special cases, however, can be solved and are shown as follows:

Case 1b-1. Sinusoidal Change in Flow Rate for Small Frequencies

If frequency w is sufficiently small, then

$$\sin \{wg(y)\} = wg(y) \quad (35)$$

The solution for $g(y)$ from equation (34) is

$$g(y) = \frac{y}{1+A} \quad (36)$$

Therefore, the response to this disturbance is exactly the same as the response to a step disturbance with a step magnitude of A . This shows that the frequency response at low frequency can be approximated by the step response.

Case 1b-2. Sinusoidal Change in Flow Rate for Large Frequencies

If w is sufficiently large, equation (34) becomes

$$g(y) = y \quad (37)$$

Equation (20) then becomes

$$\bar{\theta} = \frac{J_1(\alpha_n)}{\alpha_n} \{ (b_s - 1) e^{-\alpha_n^2 x} + 1 \} \quad (38)$$

which is the response for $a(t) = 0$. Sinusoidal disturbance of very large frequency causes no response. The results of the above two cases come from the linearity of the system.

If general solutions for sinusoidal disturbance are desired numerical solutions can be obtained.

Case 2. Simultaneous Flow Rate and Inlet Temperature Upsets With Uniform Wall Temperature

At $t = 0$, variations of fluid flow rate and inlet temperature from the steady state are applied and the fluid temperature response is predicted. Equation (20) is solved for step and sinusoidal forcing functions to flow rate and inlet temperature and then inversion of Hankel transform equation is made. As the method of obtaining solutions is similar to Case 1, only results are presented.

Case 2a. Step Change in Flow Rate and Step Change in Inlet Temperature

$$a(t) = aU(t) \quad (22)$$

$$b(t) = BU(t) \quad (39)$$

$$\theta = 2 \sum_n \frac{J_0(\alpha_n r)}{\alpha_n J_1(\alpha_n)} \left\{ (B-1) e^{-\frac{\alpha_n^2 x}{l+a}} + 1 \right\} \text{ for } t > \frac{x}{l+a} \quad (40)$$

$$\theta = 2 \sum_n \frac{J_0(\alpha_n r)}{\alpha_n J_1(\alpha_n)} \left\{ (b_s - 1) e^{-\alpha_n^2 (x-at)} + 1 \right\}$$

$$\text{for } t < \frac{x}{l+a} \quad (41)$$

Case 2b. Step Change in Flow Rate and Sinusoidal Change.
in Inlet Temperature

$$a(t) = aU(t) \quad (22)$$

$$b(t) = A \cos wt \quad (42)$$

$$\theta = 2 \sum_n \frac{J_0(\alpha_n r)}{\alpha_n J_1(\alpha_n)} \left\{ (A \cos wt - 1) e^{-\frac{\alpha_n^2 x}{l+a}} + 1 \right\}$$

$$\text{for } t > \frac{x}{l+a} \quad (43)$$

$$\theta = 2 \sum_n \frac{J_0(\alpha_n r)}{\alpha_n J_1(\alpha_n)} \left\{ (b_s - 1) e^{-\alpha_n^2 (x-at)} + 1 \right\}$$

$$\text{for } t < \frac{x}{l+a} \quad (44)$$

Case 2c. Sinusoidal Change in Flow Rate and Step Change
in Inlet Temperature

$$a(t) = A \cos wt \quad (33)$$

$$b(t) = BU(t) \quad (39)$$

Case 2c-1. (small frequencies)

$$\theta = 2 \sum_n \frac{J_0(\alpha_n r)}{\alpha_n J_1(\alpha_n r)} \left\{ (B-1) e^{-\frac{\alpha_n^2 x}{1+a}} + 1 \right\} \quad (45)$$

$$\text{for } t + \frac{A}{w} \sin wt - x > 0$$

$$\theta = 2 \sum_n \frac{J_0(\alpha_n r)}{\alpha_n J_1(\alpha_n r)} \left\{ (b_s - 1) e^{-\alpha_n^2 (x-At)} + 1 \right\} \quad (46)$$

$$\text{for } t + \frac{A}{w} \sin wt - x < 0$$

Case 2c-2. (large frequencies)

$$\theta = 2 \sum_n \frac{J_0(\alpha_n r)}{\alpha_n J_1(\alpha_n r)} \left\{ (B-1) e^{-\alpha_n^2 x} + 1 \right\} \quad (47)$$

$$\text{for } t + \frac{A}{w} \sin wt - x > 0$$

$$\theta = 2 \sum_n \frac{J_0(\alpha_n r)}{\alpha_n J_1(\alpha_n)} \{(b_s - 1) e^{-\alpha_n^2 x} + 1\}$$

for $t + \frac{A}{w} \sin wt - x < 0$ (47a)

Case 2d. Sinusoidal Changes in Flow Rate and Inlet Temperature

$$a(t) = A \cos wt \quad (48)$$

$$b(t) = A' \cos w't \quad (49)$$

Case 2d-1 (small frequencies)

$$\theta = 2 \sum_n \frac{J_0(\alpha_n r)}{\alpha_n J_1(\alpha_n)} \{(A' \cos w't - 1) e^{\frac{-\alpha_n^2 x}{1+A}} + 1\}$$

for $t + \frac{A}{w} \sin wt - x > 0$ (50)

$$\theta = 2 \sum_n \frac{J_0(\alpha_n r)}{\alpha_n J_1(\alpha_n)} \{(A' \cos w't - 1) e^{-\alpha_n^2 (x-At)} + 1\}$$

for $t + \frac{A}{w} \sin wt - x < 0$ (51)

Case 2d-2. (large frequencies)

$$\theta = 2 \sum_n \frac{J_0(\alpha_n r)}{\alpha_n J_1(\alpha_n)} (A' \cos w't - 1) e^{-\alpha_n^2 x}$$

$$\text{for } t + \frac{A}{W} \sin wt - x > 0 \quad (52)$$

$$\theta = 2 \sum_n \frac{J_0(\alpha_n r)}{\alpha_n J_1(\alpha_n)} \{ (b_s - 1) e^{-\alpha_n^2 x} + 1 \}$$

$$\text{for } t + \frac{A}{W} \sin wt - x < 0 \quad (52a)$$

Case 3. Simultaneous Flow Rate and Wall Temperature Upsets with Uniform Inlet Temperature

Case 3a. Step Change in Flow Rate and Step Change in Wall Temperature

$$a(t) = aU(t) \quad (22)$$

$$c(t) = cU(t) \quad (53)$$

$$\theta = 2 \sum_n \frac{J_0(\alpha_n r)}{\alpha_n J_1(\alpha_n)} \{ (b_s - C) e^{-\frac{\alpha_n^2 x}{1+a}} + 1 \} \text{ for } t > \frac{x}{1+a} \quad (54)$$

$$\theta = 2 \sum_n \frac{J_0(\alpha_n r)}{\alpha_n J_1(\alpha_n)} \{ (b_s - C) e^{-\alpha_n^2 (x-at)} + 1 \}$$

$$\text{for } t < \frac{x}{1+a} \quad (55)$$

Case 3b. Step Change in Flow Rate and Sinusoidal Change in Wall Temperature

$$a(t) = aU(t) \quad (22)$$

$$C(t) = A \cos wt \quad (56)$$

$$\theta = 2 \sum_n \frac{J_0(\alpha_n r)}{\alpha_n J_1(\alpha_n)} \{ (b_s - A \cos wt) e^{-\frac{\alpha_n^2 x}{1+a}} + 1 \}$$

for $t > \frac{x}{1+a}$ (57)

$$\theta = 2 \sum_n \frac{J_0(\alpha_n r)}{\alpha_n J_1(\alpha_n)} \{ (b_s - A \cos wt) e^{-\alpha_n^2 (x-at)} + 1 \}$$

for $t < \frac{x}{1+a}$ (58)

Case 3c. Sinusoidal Change in Flow Rate and Step Change in Wall Temperature

$$a(t) = a \cos wt \quad (48)$$

$$C(t) = CU(t) \quad (53)$$

Case 3c-1. (small frequencies)

$$\theta = 2 \sum_n \frac{J_0(\alpha_n r)}{\alpha_n J_1(\alpha_n)} \{ (b_s - C) e^{-\frac{\alpha_n^2 x}{1+A}} + 1 \}$$

for $t + \frac{A}{W} \sin wt - x > 0$ (59)

$$\theta = 2 \sum_n \frac{J_0(\alpha_n r)}{\alpha_n J_1(\alpha_n)} \{ (b_s - C) e^{-\alpha_n^2(x-At)} + 1 \}$$

$$\text{for } t + \frac{A}{W} \sin wt - x < 0 \quad (60)$$

Case 3c-2. (large frequencies)

$$\theta = 2 \sum_n \frac{J_0(\alpha_n r)}{\alpha_n J_1(\alpha_n)} \{ (b_s - C) e^{-\alpha_n^2 x} + 1 \} \quad (61)$$

Case 3d. Sinusoidal Change in Flow Rate and Sinusoidal Change in Wall Temperature

$$a(t) = A \cos wt \quad (48)$$

$$c(t) = C \cos w't \quad (56)$$

Case 3d-1. (small frequencies)

$$\theta = 2 \sum_n \frac{J_0(\alpha_n r)}{\alpha_n J_1(\alpha_n)} \{ (b_s - C \cos w't) e^{-\frac{\alpha_n^2 x}{1+a}} + 1 \}$$

$$\text{for } t + \frac{A}{W} \sin wt - x > 0 \quad (62)$$

$$\theta = 2 \sum_n \frac{J_0(\alpha_n r)}{\alpha_n J_1(\alpha_n)} \{ (b_s - C \cos w't) e^{-\alpha_n^2(x-At)} + 1 \}$$

$$\text{for } t + \frac{A}{W} \sin wt - x < 0 \quad (63)$$

Case 3d-2. (large frequencies)

$$\theta = 2 \sum_n \frac{J_0(\alpha_n r)}{\alpha_n J_1(\alpha_n)} \{ (b_s - C \cos w't) e^{-\alpha_n^2 x} \} \quad (64)$$

Case 4. Simultaneous Wall Temperature and Inlet Temperature Upsets with Constant Flow Rate

In this case the solution becomes much simpler because $a(t) = 0$. Equation (3) becomes for this case

$$\frac{\partial \theta}{\partial t} + \frac{\partial \theta}{\partial x} = \frac{1}{r} \frac{\partial}{\partial r} \left(r \frac{\partial \theta}{\partial r} \right) \quad (65)$$

Following through from equation (7) to equation (19) with $a(t) = 0$, one obtains the functional relationship for equation (19)

$$f(y) = y + \frac{1}{\alpha_n^2} \ln \{ \alpha_n J_1(\alpha_n) d(t) - C(t) \} \quad (66)$$

Substitute equation (66) into equation (14) with $a(t) = 0$, and obtain

$$\bar{\theta} = \frac{J_1(\alpha_n)}{\alpha_n} \{ [b(t) - C(t)] e^{-\alpha_n^2 x} + C(t) \} \quad (67)$$

Equation (67) is solved for step and sinusoidal forcing

functions to wall temperature and inlet temperature.

Case 4a. Step Change in Wall Temperature and Step Change
in Inlet Temperature

$$c(t) = CU(t)$$

$$b(t) = BU(t)$$

$$\theta = 2 \sum_n \frac{J_0(\alpha_n)}{\alpha_n J_1(\alpha_n)} \{(b-C) e^{-\alpha_n^2 x} + C\} \quad (68)$$

Case 4b. Step Change in Wall Temperature and Sinusoidal
Change in Inlet Temperature

$$c(t) = CU(t)$$

$$b(t) = D \cos wt$$

$$\theta = 2 \sum_n \frac{J_0(\alpha_n r)}{\alpha_n J_1(\alpha_n)} \{(D \cos wt - C) e^{-\alpha_n^2 x} + C\} \quad (69)$$

Case 4c. Sinusoidal Change in Wall Temperature and Step
Change in Inlet Temperature

$$c(t) = A \cos wt$$

$$b(t) = BU(t)$$

$$\theta = 2 \sum_n \frac{J_0(\alpha_n r)}{\alpha_n J_1(\alpha_n)} \{(B - A \cos wt) e^{-\alpha_n^2 x} + A \cos wt\} \quad (70)$$

Case 4d. Sinusoidal Changes in Wall Temperature and Inlet Temperature

$$c(t) = A \cos wt$$

$$b(t) = D \cos w't$$

$$\theta = 2 \sum_n \frac{J_0(\alpha_n r)}{\alpha_n J_1(\alpha_n)} \{(D \cos w't - A \cos wt) e^{-\alpha_n^2 x} + A \cos wt\} \quad (71)$$

Response to single upsets in wall temperature or inlet temperature can easily be obtained from the above equations by setting either $b(t) = b_s$ or $c(t) = 1$.

Simultaneous upsets of flow rate, inlet temperature, and wall temperature also can be obtained from equation (20) by substituting suitable expression of $a(t)$, $b(t)$, and $c(t)$. The presentation of these three simultaneous upsets will not be presented here.

Case 5. Simultaneous Flow Rate and Wall Heat Flux Upsets with Uniform Wall Heat Flux

Equation (1) describes the system, and boundary conditions to be satisfied are:

$$\begin{aligned}
1. \quad t^* &= 0, & T &= T_s \\
2. \quad x^* &= 0, & T &= T_i \\
3. \quad r^* &= 0, & \frac{\partial T}{\partial r^*} &= 0 \\
4. \quad r^* &= R, & q &= k \frac{\partial T}{\partial r^*}
\end{aligned} \tag{72}$$

Define a new dimensionless variable for temperature,

$$\theta = \frac{T - T_i}{q_s \frac{R}{k}} \tag{73}$$

θ is defined differently here than for Case 1 while other dimensionless variables are the same. Equation (3) is obtained with new variables. New boundary conditions which must be satisfied are:

$$\begin{aligned}
1. \quad t &= \theta, & \theta &= \theta_s \\
2. \quad x &= 0, & \theta &= 0 \\
3. \quad r &= 0, & \frac{\partial \theta}{\partial r} &= 0 \\
4. \quad r &= 1, & \frac{\partial \theta}{\partial r} &= -h(t)
\end{aligned} \tag{74}$$

$$\text{where } h(t) = \left. \begin{array}{l} \frac{\partial T}{\partial r^*} \\ \frac{\partial T_s}{\partial r^*} \end{array} \right|_{r^* = R}$$

Define the Hankel transform

$$\bar{\theta} = \int_0^1 \theta r J_0(\beta_n r) dr \quad (75)$$

where β_n is a root of

$$J_1(\beta_n) = 0 \quad (76)$$

where n is taken over all the possible zeroes of equation (76).

Multiplying both sides of equation (3) by $rJ_0(\beta_n r)$ and integrating with respect to r from 0 to 1,

$$\int_0^1 \frac{\partial \theta}{\partial t} r J_0(\beta_n r) dr + \int_0^1 \{1+a(t)\} \frac{\partial \theta}{\partial x} r J_0(\beta_n r) dr = \int_0^1 \frac{\partial}{\partial r} \left(r \frac{\partial \theta}{\partial r} \right) J_0(\beta_n r) dr \quad (77)$$

Integrating the right sides of equation (77) by parts gives

$$\frac{\partial \bar{\theta}}{\partial t} + \{1+a(t)\} \frac{\partial \bar{\theta}}{\partial x} + \beta_n^2 \bar{\theta} = -J_0(\beta_n) h(t) \quad (78)$$

Equations (74), (75), and (76) are used to obtain equation (78). Equation (78) is solved by the characteristic method

used in Case 1.

From equation (78), we obtain an equation similar to equation (11):

$$dt = \frac{dx}{1+a(t)} = - \frac{d\bar{\theta}}{\beta_n^2 \bar{\theta} + J_0(\beta_n)h(t)} \quad (78a)$$

Following the procedure used in Case 1, the general solution for $\bar{\theta}$ subjected to wall heat flux and flow rate is obtained.

$$\bar{\theta} = \frac{h(t)J_0(\beta_n)}{\beta_n^2} \left\{ \exp \left\{ \beta_n^2 \int_{g(y)}^t a(\tau)d\tau - \beta_n^2 x \right\} - 1 \right\} \quad (79)$$

Case 5a. Step Changes in Flow Rate and Wall Heat Flux

$$a(t) = aU(t) \quad (22)$$

$$h(t) = hU(t) \quad (80)$$

Substitute equations (22) and (80) into equation (79) and solve equation (79) for $\bar{\theta}$. As in the case of Case 1 it is easier to solve equation (79) after $g(y)$ is obtained from equation (18).

$$g(t+at-x) = t - \frac{x}{1+a}$$

Substitute equations (25) and (80) into equation (79) and

equation (79) can be solved for $\bar{\theta}$.

$$\bar{\theta} = \frac{hJ_0(\beta_n)}{\beta_n^2} \left\{ e^{-\frac{\beta_n^2 x}{1+a}} - 1 \right\} \text{ for } t > \frac{x}{1+a} \quad (81)$$

$$\bar{\theta} = \frac{hJ_0(\beta_n)}{\beta_n^2} \left\{ e^{-\beta_n^2(x-at)} - 1 \right\} \text{ for } t < \frac{x}{1+a} \quad (82)$$

When β_n is a root of equation (76) and if θ can be represented in the range of $0 < r < 1$ by

$$\theta(x, r, t) = \sum_n D_n J_0(\beta_n r) \quad (83)$$

then the coefficients D_n are given

$$D_n = \frac{2}{J_0^2(\beta_n)} \int_0^1 \theta r J_0(\beta_n r) dr = \frac{2\bar{\theta}}{J_0^2(\beta_n)} \quad (84)$$

Therefore, inversion of the Hankel transform in equation (84) gives,

$$\theta(x, r, t) = 2 \sum_n \frac{J_0(\beta_n r)}{J_0^2(\beta_n)} \bar{\theta} \quad (85)$$

Substituting equations (81) and (82) into equation (85) gives

$$\theta = 2 \sum_n \frac{h J_0(\beta_n r)}{J_0(\beta_n) \beta_n^2} \left\{ e^{-\frac{\beta_n^2 x}{1+a}} - 1 \right\} \text{ for } t > \frac{x}{1+a} \quad (86)$$

$$\theta = 2 \sum_n \frac{h J_0(\beta_n r)}{\beta_n^2 J_0(\beta_n)} \left\{ e^{-\beta_n^2 (x-at)} - 1 \right\} \text{ for } t < \frac{x}{1+a} \quad (87)$$

Case 5b. Step Change in Flow Rate and Sinusoidal Change
in Wall Heat Flux

$$a(t) = aU(t) \quad (22)$$

$$h(t) = H \cos wt \quad (88)$$

$$\theta = 2 \sum_n \frac{H \cos wt J_0(\beta_n r)}{\beta_n^2 J_0(\beta_n)} \left\{ e^{-\frac{\beta_n^2 x}{1+a}} - 1 \right\} \text{ for } t > \frac{x}{1+a} \quad (89)$$

$$\theta = 2 \sum_n \frac{H \cos wt J_0(\beta_n r)}{\beta_n^2 J_0(\beta_n)} \left\{ e^{-\beta_n^2 (x-at)} - 1 \right\} \text{ for } t < \frac{x}{1+a} \quad (90)$$

Case 5c. Sinusoidal Change in Flow Rate and Step Change in
Wall Heat Flux

$$a(t) = A \cos wt$$

$$h(t) = hU(t)$$

Case 5c-1. (small frequencies)

$$\theta = 2 \sum_n \frac{hJ_0(\beta_n r)}{\beta_n^2 J_0(\beta_n)} \left\{ e^{-\frac{\beta_n^2 x}{1+A}} - 1 \right\} \text{ for } t + \frac{A}{w} \sin wt - x > 0 \quad (91)$$

$$\theta = 2 \sum_n \frac{hJ_0(\beta_n r)}{\beta_n^2 J_0(\beta_n)} \left\{ e^{-\beta_n^2 (x-At)} - 1 \right\} \text{ for}$$

$$t + \frac{A}{w} \sin wt - x < 0 \quad (92)$$

Case 5c-2. (large frequencies)

$$\theta = 2 \sum_n \frac{hJ_0(\beta_n r)}{\beta_n^2 J_0(\beta_n)} \left\{ e^{-\beta_n^2 x} - 1 \right\} \quad (93)$$

Case 5d. Sinusoidal Changes in Flow Rate and Wall Heat Flux

$$a(t) = A \cos wt$$

$$h(t) = H \cos w't$$

Case 5d-1. (small frequencies)

$$\theta = 2 \sum_n \frac{H \cos w't J_0(\beta_n r)}{\beta_n^2 J_0(\beta_n)} \left\{ e^{-\frac{\beta_n^2 x}{1+a}} - 1 \right\} \text{ for } t + \frac{A}{w} \sin wt - x > 0 \quad (94)$$

$$\theta = 2 \sum_n \frac{H \cos w't J_0(\beta_n r)}{\beta_n^2 J_0(\beta_n)} \{ e^{-\beta_n^2(x-At)} - 1 \}$$

for $t + \frac{A}{w} \sin wt - x < 0$ (95)

Case 5d-2. (large frequencies)

$$\theta = 2 \sum_n \frac{H \cos w't J_0(\beta_n r)}{\beta_n^2 J_0(\beta_n)} \{ e^{-\beta_n^2 x} - 1 \}$$

(96)

Responses to single upsets of wall heat flux or flow rate can easily be obtained from above equations by setting either $a(t) = 0$, or $h(t) = 1$. For instance, for a step change in flow rate with constant wall heat flux

$$a(t) = AU(t), \quad h(t) = 1$$

From equations (86) and (87) the following two equations are obtained.

$$\theta = 2 \sum_n \frac{J_0(\beta_n r)}{\beta_n^2 J_0(\beta_n)} \{ e^{-\frac{\beta_n^2 x}{1+a}} - 1 \} \text{ for } t > \frac{x}{1+a}$$

(86a)

$$\theta = 2 \sum_n \frac{J_0(\beta_n r)}{\beta_n^2 J_0(\beta_n)} \{ e^{-\beta_n^2(x-at)} - 1 \} t < \frac{x}{1+a}$$

(87a)

For a step change in wall heat flux with constant flow rate

$$a(t) = 0$$

$$h(t) = hU(t)$$

From equations (86) and (87) following equation is obtained.

$$\theta = 2 \sum_n \frac{hJ_0(\beta_n r)}{\beta_n^2 J_0(\beta_n)} \{ e^{-\beta_n^2 x} - 1 \} \quad (86b)$$

Case 6. Axial Varying Wall Temperature Upsets

At $t = 0$, it is assumed that wall temperature variations which are a function of axial distance are applied on the wall. Equation (1) and boundary conditions given by equation (2) describe the system.

Dimensionless variables θ , x , t , and r are defined in equation (24). Note that T_w is a function of axial distance for this case. In these dimensionless variables equation (3) is obtained. Boundary conditions to be satisfied are:

1. $t = 0, \quad \theta = \theta_s$
2. $x = 0, \quad \theta = b(t) \quad (97)$
3. $r = 0, \quad \frac{\partial \theta}{\partial r} = 0$
4. $r = 1, \quad \theta = c(x)$

where $b(t) = T_i(t)/T_{ws}$

$$c(x) = T_w(x)/T_{ws} \quad (98)$$

Following the procedure of Case 1, one obtains the general solution for $\bar{\theta}$ as follows:

$$\bar{\theta} = \frac{J_1(\alpha_n)}{\alpha_n} \{b(t) - c(x)\} \exp \left\{ \alpha_n^2 \int_0^t a(\tau) d\tau - \alpha_n^2 x \right\} + \frac{J_1(\alpha_n)}{\alpha_n} c(x) \quad (99)$$

Note that equation (99) for an axial disturbance in wall temperature is identical to equation (20) for a time disturbance in wall temperature except $c(t)$ is replaced by $c(x)$. Therefore, the response of an axial varying forcing function to wall temperature upsets would give the same result as time varying forcing functions except $c(t)$ is replaced by $c(x)$.

Case 7. Axial Varying Wall Heat Flux Upsets

At $t^* = 0$, wall heat flux variation which are a function of axial distance are applied on the wall. Equation (1) and

boundary conditions given by equation (72) describe the system.

Dimensionless variables θ , x , t , and r are defined in equation (73) and (2a). In terms of these dimensionless variables equation (3) is obtained. Boundary conditions to be satisfied are:

$$\begin{aligned}
 1. \quad t = 0, \quad \theta &= \theta_s \\
 2. \quad x = 0, \quad \theta &= b(t) \\
 3. \quad r = 0, \quad \frac{\partial \theta}{\partial r} &= 0 \\
 4. \quad r = 1, \quad \theta &= -h(x)
 \end{aligned} \tag{100}$$

where $b(t) = T_i(t)/T_{ws}$

$$h(x) = \left. \begin{array}{l} \frac{\partial T}{\partial r^*} \\ \frac{\partial T_s}{\partial r^*} \end{array} \right|_{r^* = R} \tag{101}$$

Following the procedure of Case 5, one obtains the general solution for $\bar{\theta}$ which is similar to equation (79).

$$\bar{\theta} = \frac{h(x)J_0(\beta_n)}{\beta_n^2} \left\{ \exp \beta_n^2 \left\{ \int_0^t a(\tau) d\tau - x \right\} - 1 \right\} \tag{102}$$

One can see that the response of axial varying forcing function to wall heat flux would be identical to the response to time varying forcing functions to wall heat flux except $h(t)$ is replaced by $h(x)$.

DISCUSSION OF EXPERIMENTAL AND THEORETICAL RESULTS

Experimental data are plotted with theoretical models for step changes in liquid flow rate with uniform wall heat-fluxes. Temperatures of the liquid at different radial positions are plotted in Figs. 3 through 12. Experimental and theoretical temperature response is plotted against reduced radius in Fig. 13 with time as a parameter. Theoretical temperature response to transient inlet temperature and transient flow changes with uniform wall temperature are plotted in Figs. 14 and 15.

In theory, the response must be complete after an elapsed time of L/u , where L is the Heat-exchanger length and u is the fluid velocity after upset. Thus, L/u divides the response plane into two time domains. After an elapsed time of L/u , the dynamic response to a flow-rate upset is theoretically no longer dependent on time. Actual response is usually slightly longer than L/u due to nonlinearities in the system. It was assumed in this study that the fluid

traveled at its average velocity. Thus, it was assumed that each element of fluid required the same length of time to pass through the heat exchanger, regardless of its radial position. Average velocity of the fluid was obtained experimentally by measuring the volumetric flow rate. In actual laminar flow in a tube, the fluid velocity at the wall is very small compared with the average velocity. Hence, L/u of the fluid element at the wall is larger than that of fluid with average velocity. The opposite phenomenon occurs at the center of the tube because the velocity at the center of the tube is very large compared with the average velocity. The average fluid velocity in isothermal laminar flow in a tube occurs at the reduced radius of 0.707. For non-isothermal flow it cannot be determined where the average velocity occurs unless a precise velocity profile is known. Figures 3 through 12 show that there are differences between the speed of response of experimental and theoretical data. At certain radial positions the degree of difference varies more consistently than at others. As expected, Figs. 3 through 12 show that the speed of response of experimental data is slower at the wall and faster at the center than that of the theoretical data. However, the speed of response of experimental and theoretical data agree very well at a reduced radius of approximately from 0.7 to 0.8. It has been found

by Boelter⁽¹²⁾ that theoretical solutions assuming a flat average velocity profile agree better with experimental data than theoretical solutions that assume a parabolic velocity profile. This discrepancy has been explained by Boelter on the basis of changes in the physical properties, resulting in natural convection. Kirkbride and McCabe⁽⁸⁾, in their study of heat transfer to liquids in viscous flow, also found that the parabolic velocity profile introduced an error in their study. They found that not only natural convection but also radial flow of fluid caused the distortion of the velocity profile. This radial flow of fluid was generated by the temperature gradient due to the changing of the fluid viscosity in the layer near the wall. Since the actual velocity profile is not known for non-isothermal condition, it turns out that assuming a constant average velocity is not a stronger assumption than assuming a parabolic velocity profile. Oliver⁽¹³⁾, in his study of the effect of natural convection on viscous-flow heat transfer in horizontal tubes, presented the qualitative velocity profile shown in Fig. 16 when the natural convection assisted the forced flow. When the effect of natural convection is not negligible, an additional complication is added to the theoretical model to be used in predicting the dynamic temperature response of a laminar-flow heat exchanger. The

velocity profile is no longer predictable for this case.

The accuracy of the models depended greatly on knowledge of the steady-state conditions since steady-state experimental data were used to evaluate the wall heat-flux. An average temperature was obtained from a graphical integration of a steady-state temperature profile. The heat absorbed by the liquid, $WC_p(T_{La}-T_i)$ was obtained by the heat balance over the heat-exchanger length. This value was used for the wall heat-flux. In steady-state laminar-flow heat exchanger a uniform wall heat-flux may be obtainable. In an unsteady-state laminar-flow flow-forced heat exchanger it may be difficult to obtain a uniform wall heat-flux. Experimentally, wall heat-flux may be calculated from the term $WC_p(T_{La}-T_i)$ where this term can also be assumed to equal $h_a S \Delta T_a$, where the heat transfer coefficient is dependent on the fluid velocity. In laminar flow the heat transfer coefficient is dependent on the fluid velocity to the one-third power. Therefore, when a fluid flow-rate change is made the heat transfer coefficient changes. The temperature difference, ΔT_a , also changes. Hence, it is known that the heat flux calculated by the heat balance does not stay constant throughout the unsteady-state period. There is no simple way of calculating how the wall heat-flux would change in an unsteady-state laminar-flow flow-forced heat exchanger. However, for this study the

difference between the wall heat-flux calculated from the initial and final steady-state temperature profiles investigated was found to be small and negligible. A difference was found between the electrical heat input and wall heat-flux calculated by the experimental heat balance. The difference was negligible for the wall heat-flux of 817 Btu/hr ft², and 13 and 34 percent for cases of wall heat-fluxes of 1115 and 1900 Btu/ft²·hr. This variance was expected since it was felt that the lack of perfect insulation which caused heat loss could never be fully eliminated except for the case of the low wall heat-flux.

The ratio of N_{Gr}/N_{Re}^2 has been found to be very significant for determining the range of experimental conditions that give good experimental laminar-flow dynamic response data. N_{Gr} and N_{Re} are defined in nomenclature, but it must be noted that N_{Re} was defined on the basis of the heat exchanger length L for this ratio instead of the diameter D . When the physical properties of liquids were constant and the heat-exchanger length was fixed, the pertinent variables which determine the ratio N_{Gr}/N_{Re}^2 are $\Delta T/u^2$. Many engineers have found that the parameter N_{Gr}/N_{Re}^2 is of fundamental importance in determining the predominant effect of natural or forced convection. Table 1 gives the range of suggested values of the ratio N_{Gr}/N_{Re}^2 at which it is permissible to neglect one mode of heat transfer for the other.

Table 1

Author	Forced convection predominates	Natural convection predominates
Acrivos ⁽¹⁴⁾	$N_{Gr}/N_{Re}^2 < 0.02$	$N_{Gr}/N_{Re}^2 > 100$
Kreith ⁽¹⁵⁾	$N_{Gr}/N_{Re}^2 < 1$	$N_{Gr}/N_{Re}^2 > 1$
Sparrow and Gregg ⁽¹⁶⁾	$N_{Gr}/N_{Re}^2 < 0.061$	

As shown in Table 3, the criteria determining the predominant effect of natural or forced convection vary from author to author. Since the present theoretical model did not include the effect of natural convection, it was necessary to keep the ratio N_{Gr}/N_{Re}^2 as low as possible. The range of the ratio N_{Gr}/N_{Re}^2 for this experimental study was from 2×10^{-4} to 2. With constant physical properties of liquids there are two pertinent variables which can vary the ratio N_{Gr}/N_{Re}^2 in the present experimental study. They are the fluid velocity and the temperature difference from the inlet to the outlet of the heat exchanger. Note that this temperature difference is proportional to the wall heat-flux. Therefore, there are limitations on the wall heat-flux and the fluid velocity to keep the ratio N_{Gr}/N_{Re}^2 under certain desired limits. For a fixed fluid velocity there is a maximum wall heat-flux, and

for a fixed wall heat-flux there is a minimum fluid velocity. The maximum wall heat-flux applied in the experiment was 1900 Btu/ft²hr for Run 1. The minimum fluid velocity was 0.1875 ft/sec for Run 3. For the range of conditions for which data are presented in this dissertation very little indication of error due to natural convection was indicated. With N_{Gr}/N_{Re}^2 of 2 for Run 9, the maximum ratio presented for the experimental study, the recorder gave temperature fluctuations of 2°F. However, in determining the range of conditions that gave suitable data, the indication of natural convection was found to be very significant when the ratio N_{Gr}/N_{Re}^2 was greater than 10 based on random behavior of fluid temperature response.

In the comparison of Figs. 4 and 5, 6 and 7, and 11 and 12, it may be observed that the magnitude of flow-rate upsets has a significant effect on the transient temperature response results. Figs. 4, 7, and 12 show better agreement between theoretical and experimental data than Figs. 5, 6, and 11. The former three runs had flow-rate upsets of 65, 47, and 32 percent departures from the initial steady state. The latter three runs had flow-rate upsets of 125, 97, and 155 percent departures from the initial steady state. Experimental data show that the actual speed of response for the latter three cases is slower than that of theoretical

Figure 3. Experimental and theoretical fluid temperature response to transient flow changes between 0.273 ft/sec and 0.467 ft/sec with uniform wall heat-flux (Run 1)^a

Legend: ——— Theoretical solution

Experimental data

- r = 1.0
- △ r = 0.91
- r = 0.79

^aSee Table 2 for conditions of Run 1

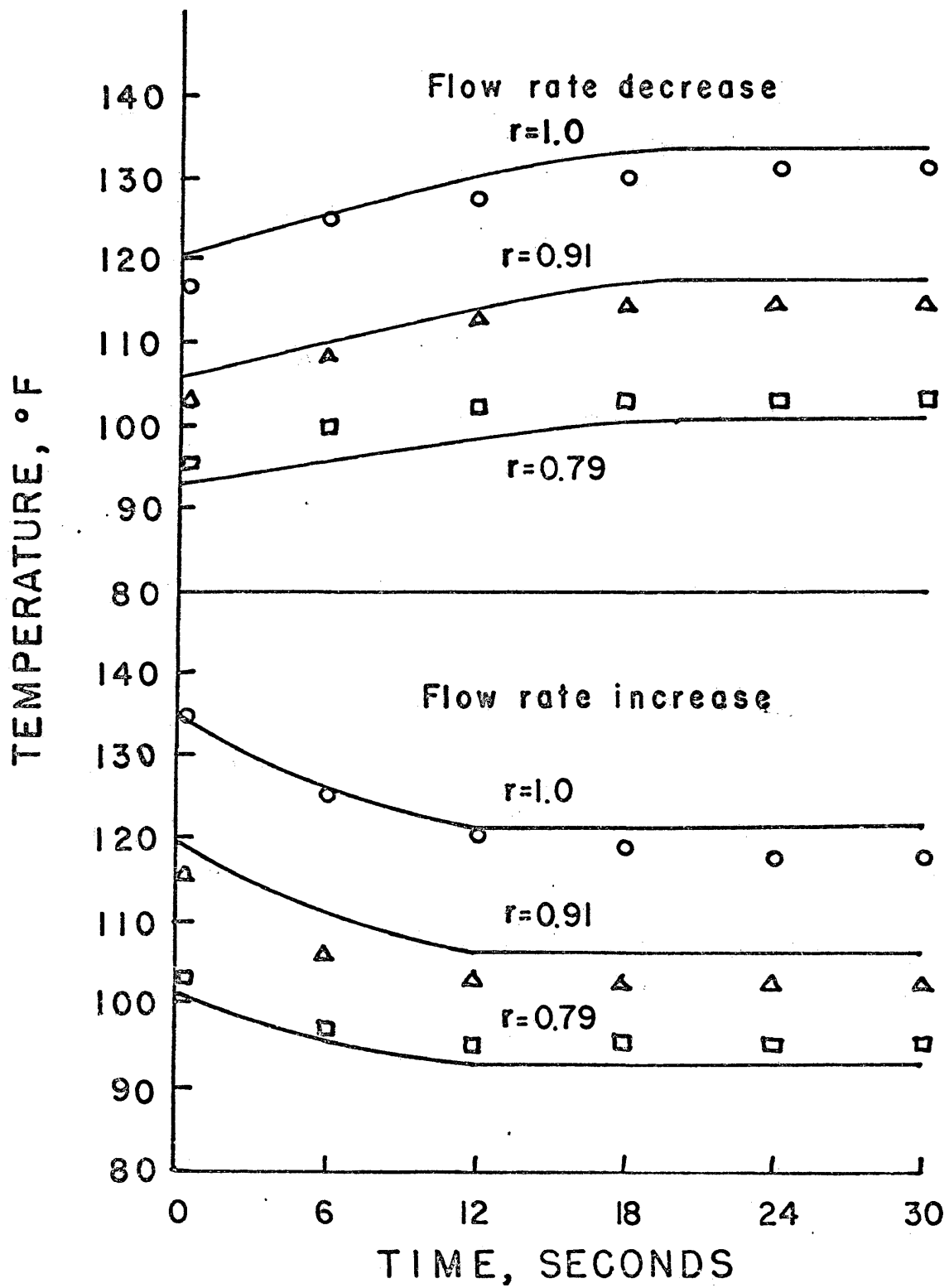


Figure 4. Experimental and theoretical fluid temperature response to transient flow changes between 0.188 ft/sec and 0.309 ft/sec with uniform wall heat-flux (Run 2)^a

Legend: — Theoretical solution

Experimental data

- r = 1.0
- △ r = 0.86
- r = 0.75
- ⊙ r = 0.41

^aSee Table 2 for conditions of Run 2

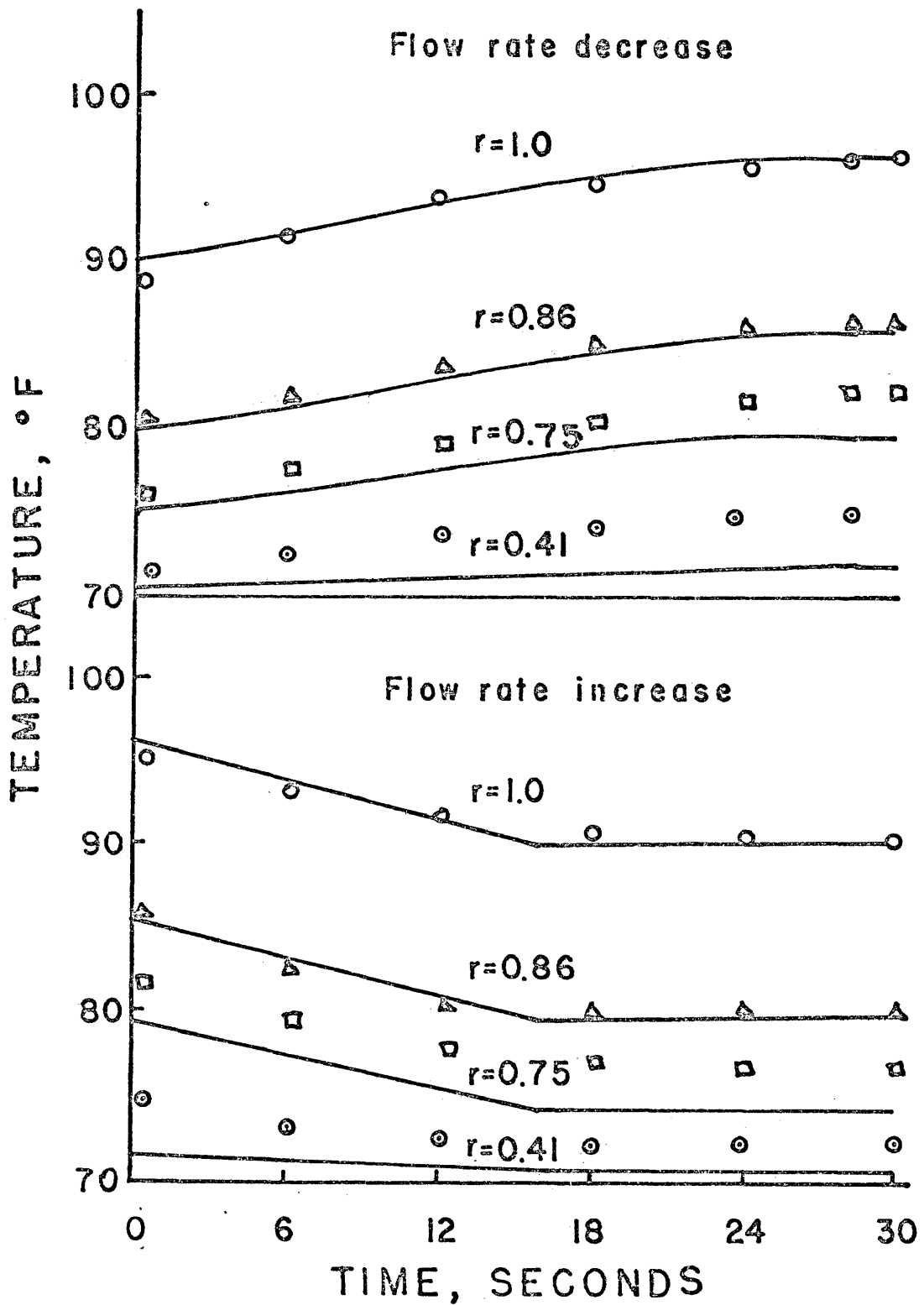


Figure 5. Experimental and theoretical fluid temperature response to transient flow changes between 0.188 ft/sec and 0.42 ft/sec with uniform wall heat-flux (Run 3)^a

Legend: — Theoretical solution
Experimental data

- r = 1.0
- △ r = 0.87
- r = 0.72
- ⊙ r = 0.28

^aSee Table 2 for conditions of Run 3

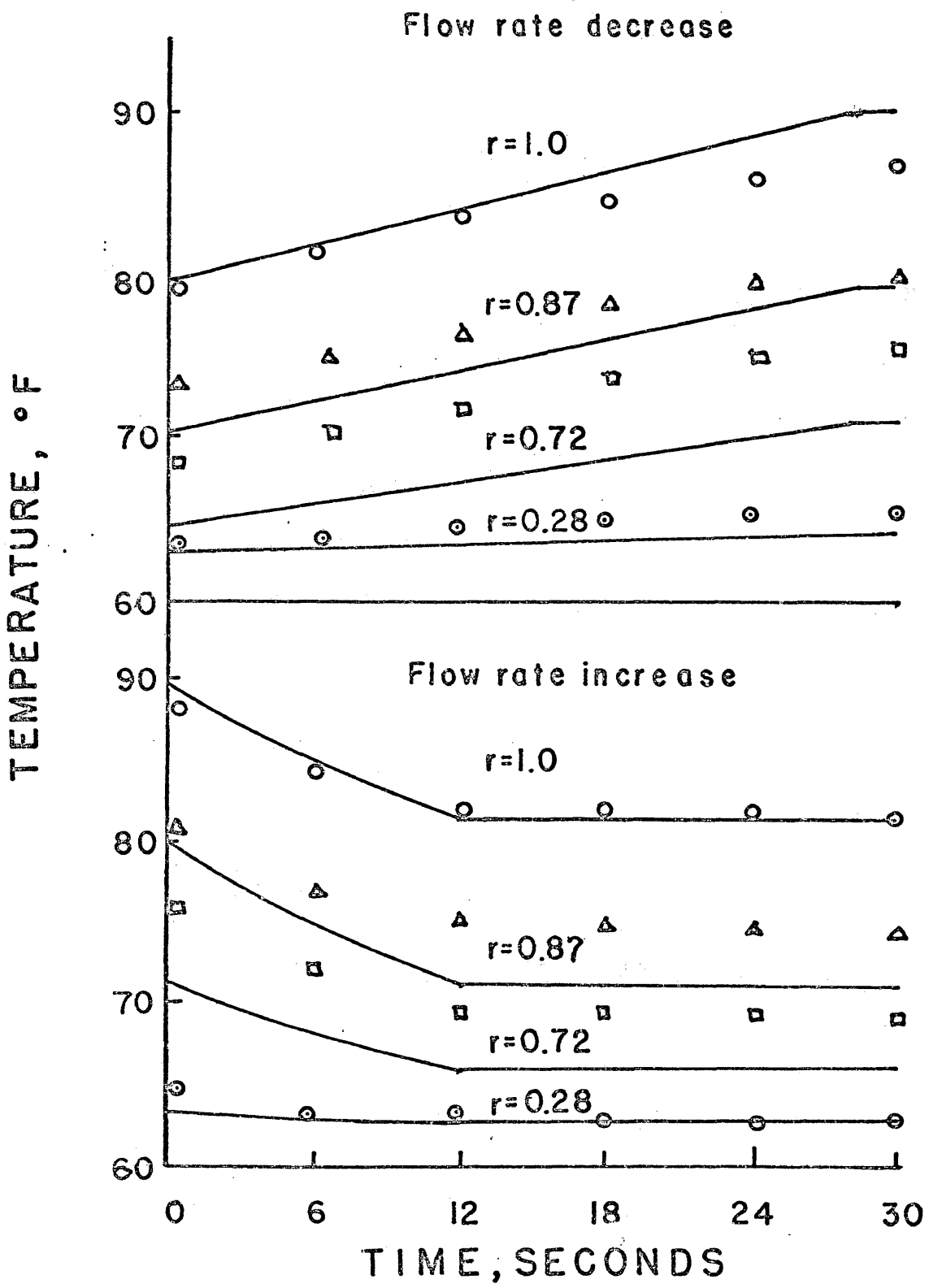


Figure 6. Experimental and theoretical fluid temperature response to transient flow changes between 0.228 ft/sec and 0.448 ft/sec with uniform wall heat-flux (Run 4)^a

Legend: — Theoretical solution
Experimental data

- r = 1.0
- △ r = 0.85
- r = 0.62

^aSee Table 2 for conditions of Run 4

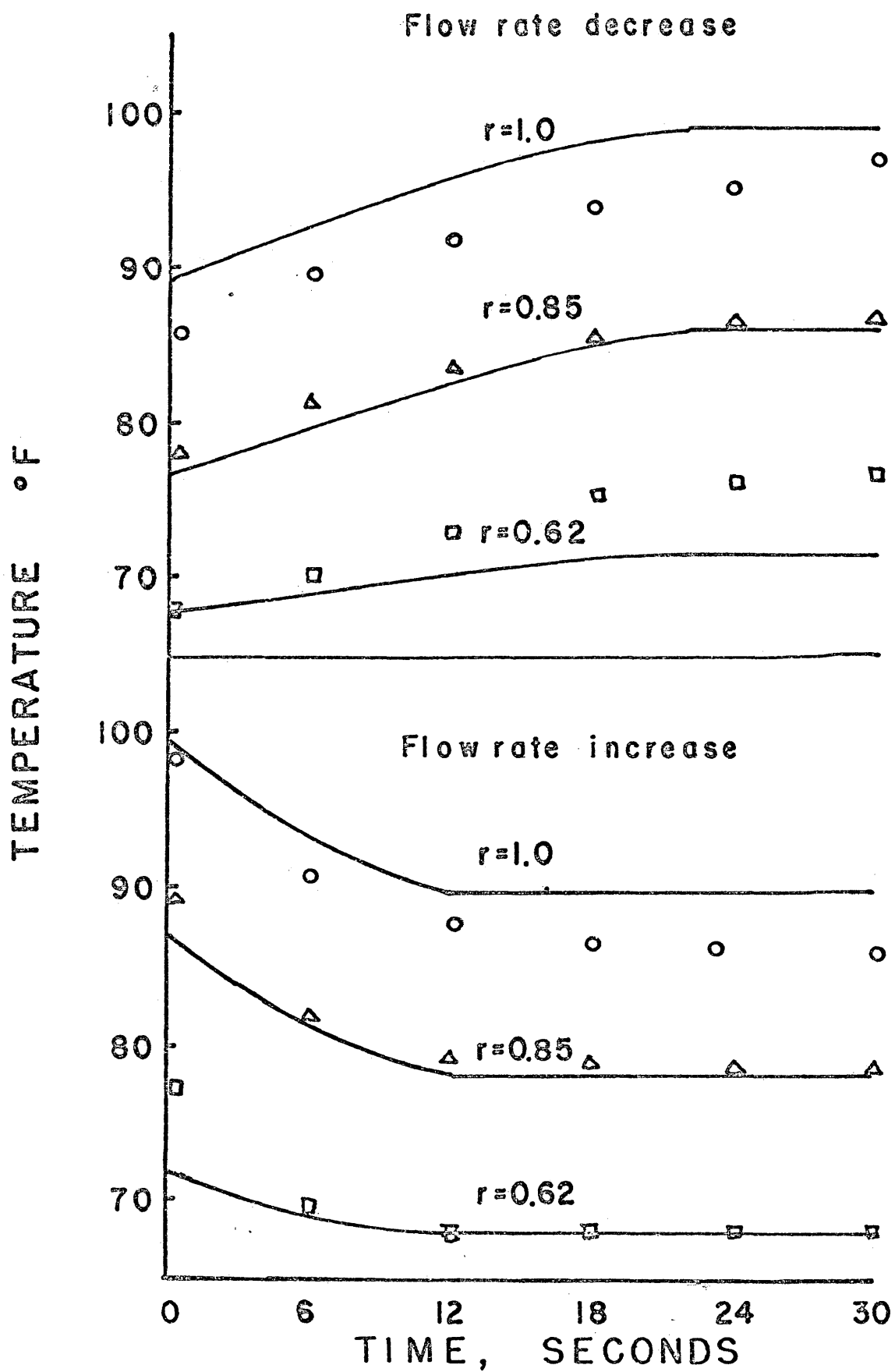


Figure 7. Experimental and theoretical fluid temperature response to transient flow changes between 0.228 ft/sec and 0.337 ft/sec with uniform wall heat-flux (Run 5)^a

Legend: — Theoretical solution

Experimental data

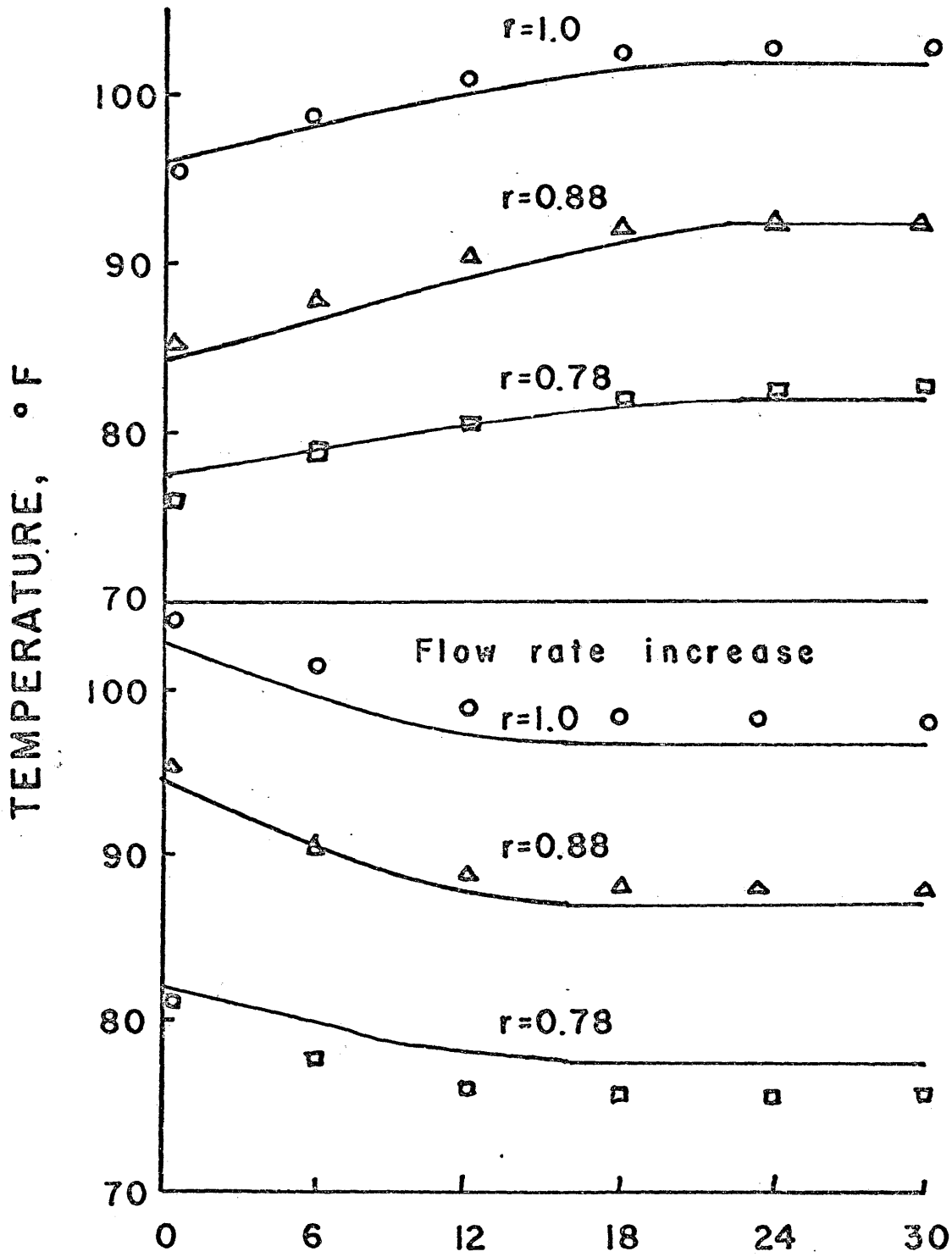
○ r = 1.0

△ r = 0.88

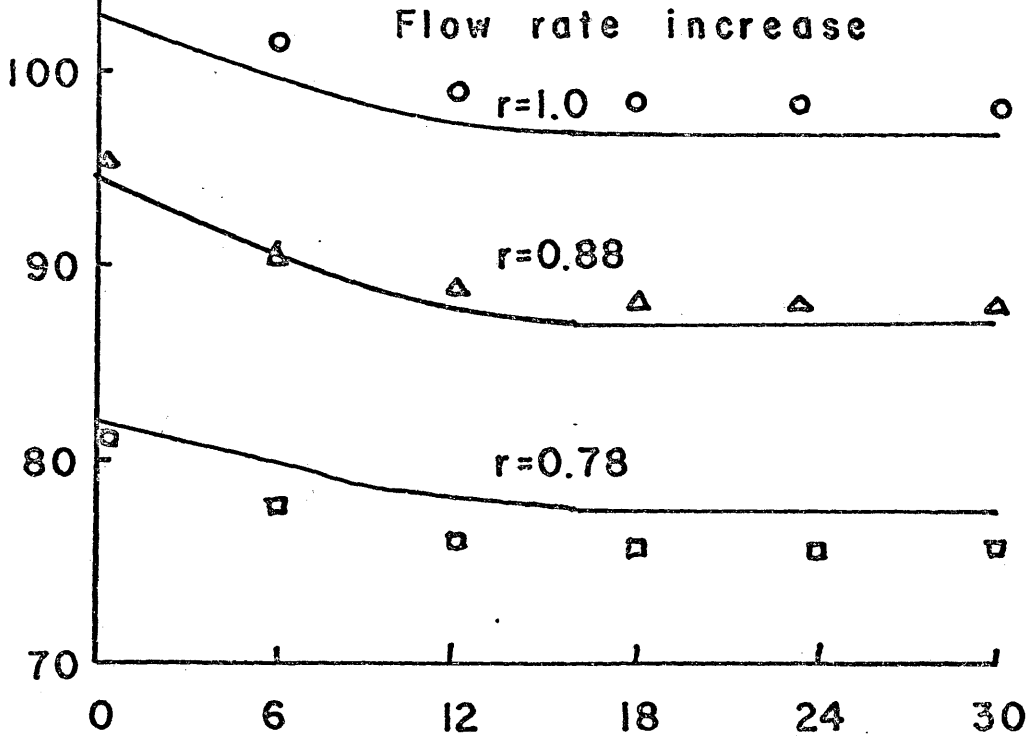
□ r = 0.78

^aSee Table 2 for conditions of Run 5

Flow rate decrease



Flow rate increase



TIME, SECONDS

Figure 8. Experimental and theoretical fluid temperature response to transient flow changes between 0.289 ft/sec and 0.438 ft/sec with uniform wall heat-flux (Run 6)^a

Legend: ——— Theoretical solution
Experimental data

- r = 1.0
- △ r = 0.85
- r = 0.76

^aSee Table 2 for conditions of Run 6

Flow rate decrease

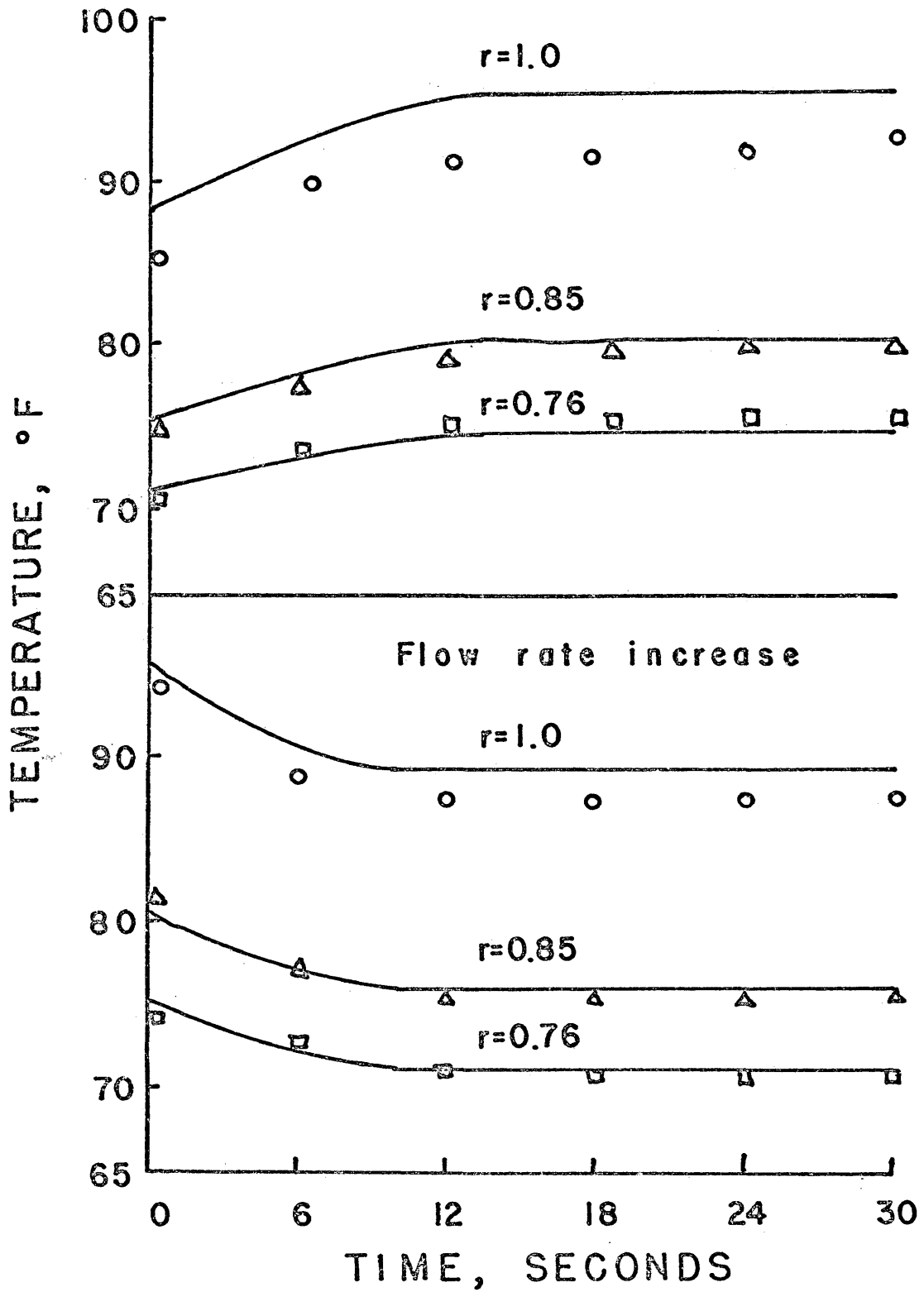
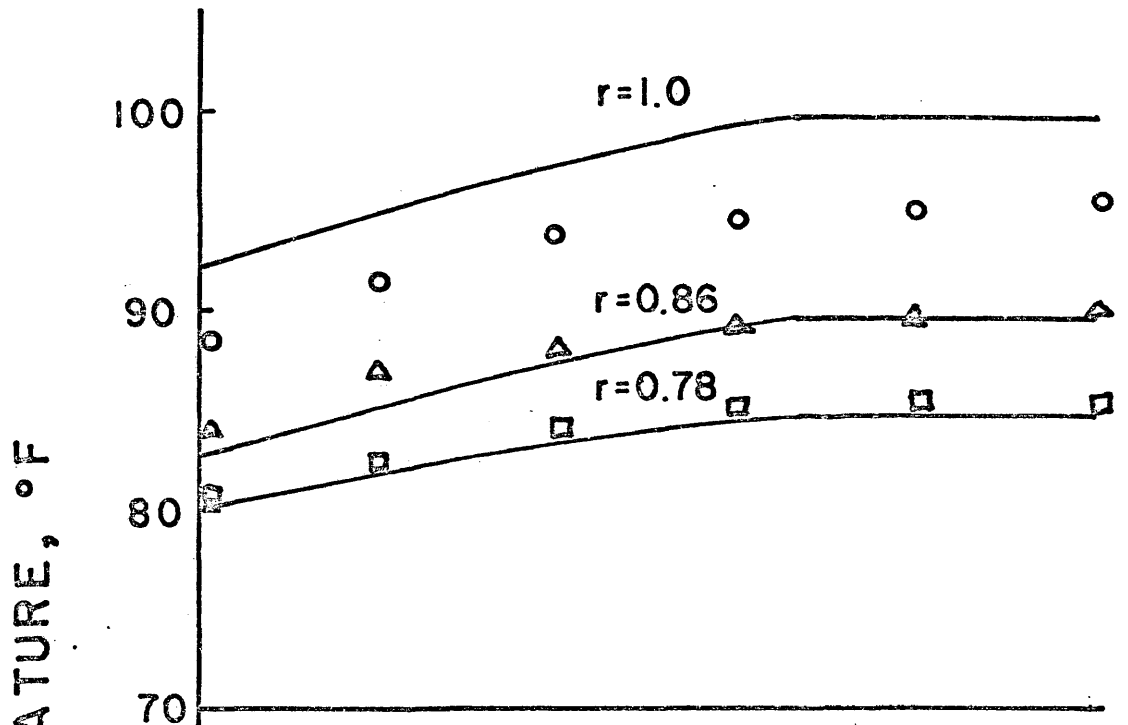


Figure 9. Experimental and theoretical fluid temperature response to transient flow changes between 0.269 ft/sec and 0.568 ft/sec with uniform wall heat-flux (Run 7)^a

Legend: — Theoretical solution
Experimental data
○ r = 1.0
△ r = 0.86
□ r = 0.78

^aSee Table 2 for conditions of Run 7

Flow rate decrease



Flow rate increase

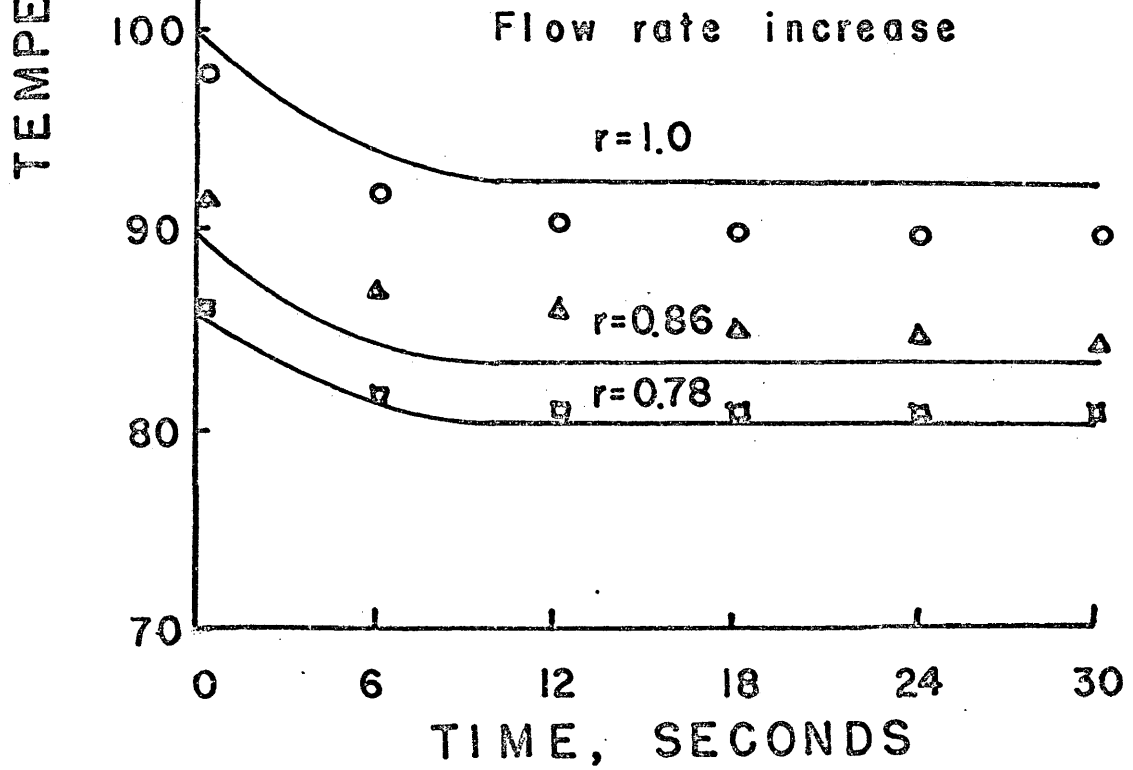


Figure 10. Experimental and theoretical fluid temperature response to transient flow changes between 0.269 ft/sec and 0.371 ft/sec with uniform wall heat-flux (Run 8)^a

Legend: — Theoretical solution

Experimental data

○ r = 1.0

⊙ r = 0.9

△ r = 0.81

^aSee Table 2 for conditions of Run 8

Flow rate decrease

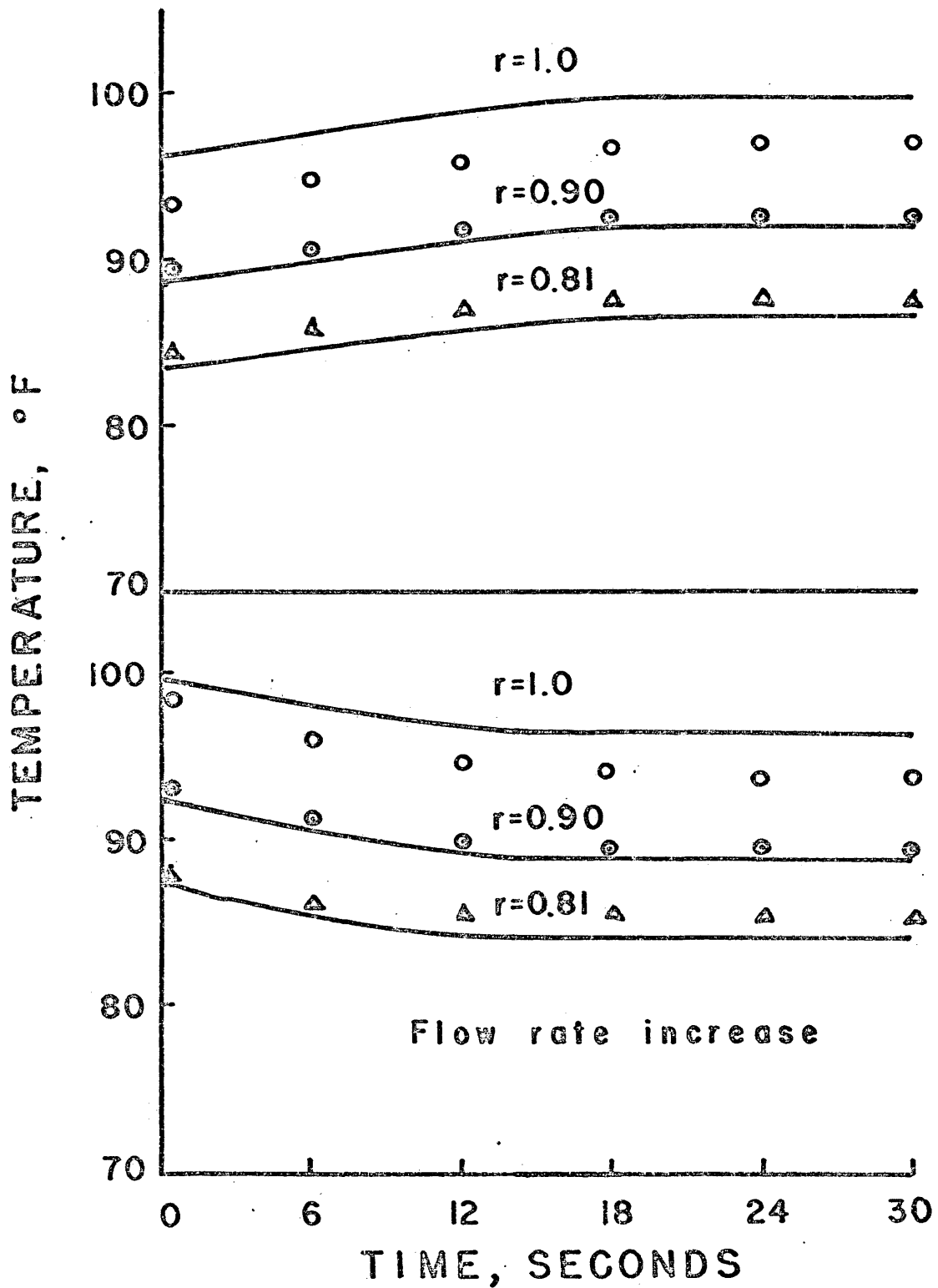


Figure 11. Experimental and theoretical fluid temperature response to transient flow changes between 0.269 ft/sec and 0.685 ft/sec with uniform wall heat-flux (Run 9)^a

Legend: — Theoretical solution
Experimental data

- r = 1.0
- △ r = 0.94
- r = 0.47

^aSee Table 2 for conditions of Run 9

Flow rate decrease

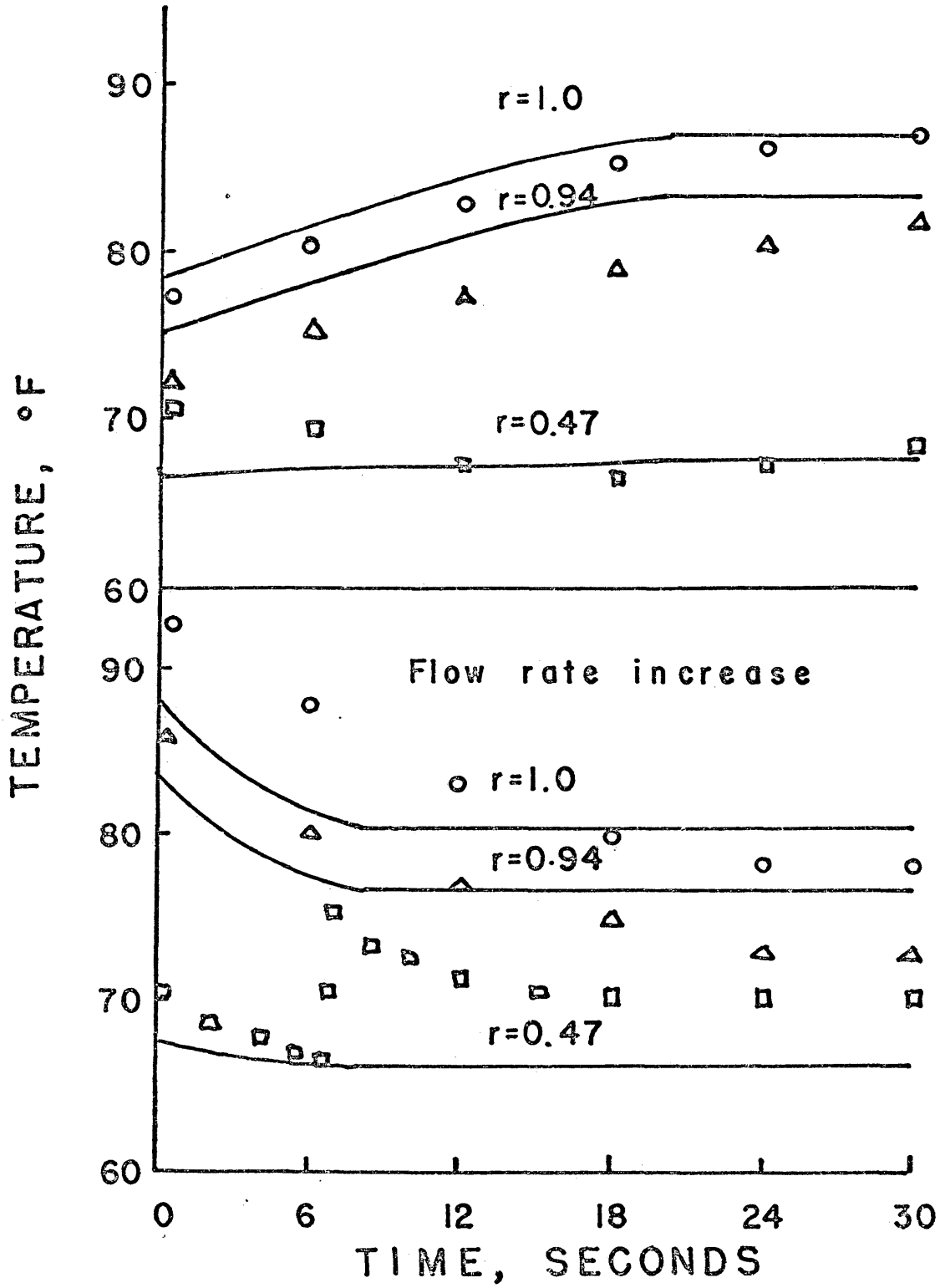


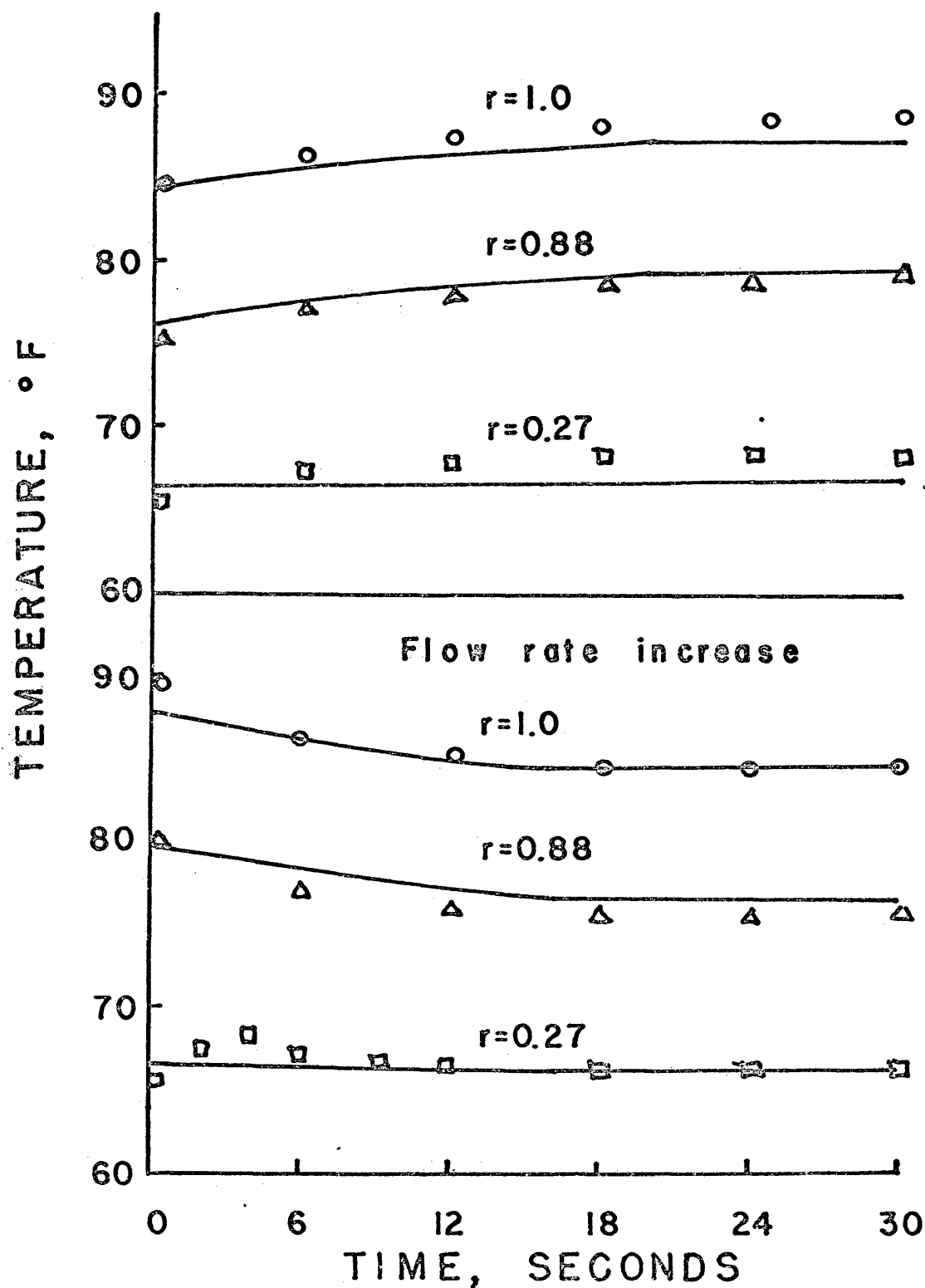
Figure 12. Experimental and theoretical fluid temperature response to transient flow changes between 0.269 ft/sec and 0.353 ft/sec with uniform wall heat-flux (Run 10)^a

Legend: — Theoretical solution
Experimental data

- r = 1.0
- △ r = 0.88
- r = 0.27

^aSee Table 2 for conditions of Run 10

Flow rate decrease



data. It is important to note that even though no linearization in the model was made, the model showed poor agreement with experimental data when high magnitudes of flow-rate upsets were applied. It was felt that one or more of the following factors were prominent reasons for poor agreement with experimental and theoretical data for large flow upsets: (1) When big step-changes in flow rate are made, the boundary condition of a uniform wall heat-flux is not as good an assumption as for small flow changes due to the change of the heat-transfer coefficient. (2) When big step changes in flow rate are made, fluid elements that do not stay in stream-line motion have turbulent mixing. (3) Nonlinearities of the actual physical system due to changes of physical properties become more prominent after big step changes in flow rate.

A very important experimental factor was the accuracy of radial temperature measurement. In this experimental study the temperature was measured at different radial positions with a thermocouple which protruded from the wall of the exchanger tube at the outlet. In this way it was possible to obtain an accurate measurement of the radial positions where fluid temperature response was measured. The radial positions were measured with a micrometer mounted parallel to the thermocouple. However, a small error was introduced into the temperature measurement due to thermal

conduction along the thermocouple wire from the wall or fluid near the thermocouple junction. This error could have been avoided by measuring fluid temperature response at different radial positions from a tee in the end of the exchanger tube rather than from the side, but it was felt that this would make it difficult to determine radial thermocouple positions accurately. In the measurement of the fluid temperature from the wall, significant thermal conduction error exists when fluid temperature is measured near the wall from which the thermocouple protruded. In this case, the temperature difference between the thermocouple junction and the wall or heating elements is at least 100°F , creating the potential for significant measuring errors of several degrees. Due to the varying temperature gradients it is very difficult to calculate these errors accurately. However, by measuring fluid temperatures at radial positions on the opposite side of the tube from which the thermocouple protrudes, it is possible to reduce the thermal conduction error. At these positions the thermocouple wire near the thermocouple junction is in contact with fluid similar in temperature to the fluid temperature being measured. No large temperature differences exist such as when the thermocouple junction is near the wall. Therefore, the thermocouple junction temperature is only slightly affected by

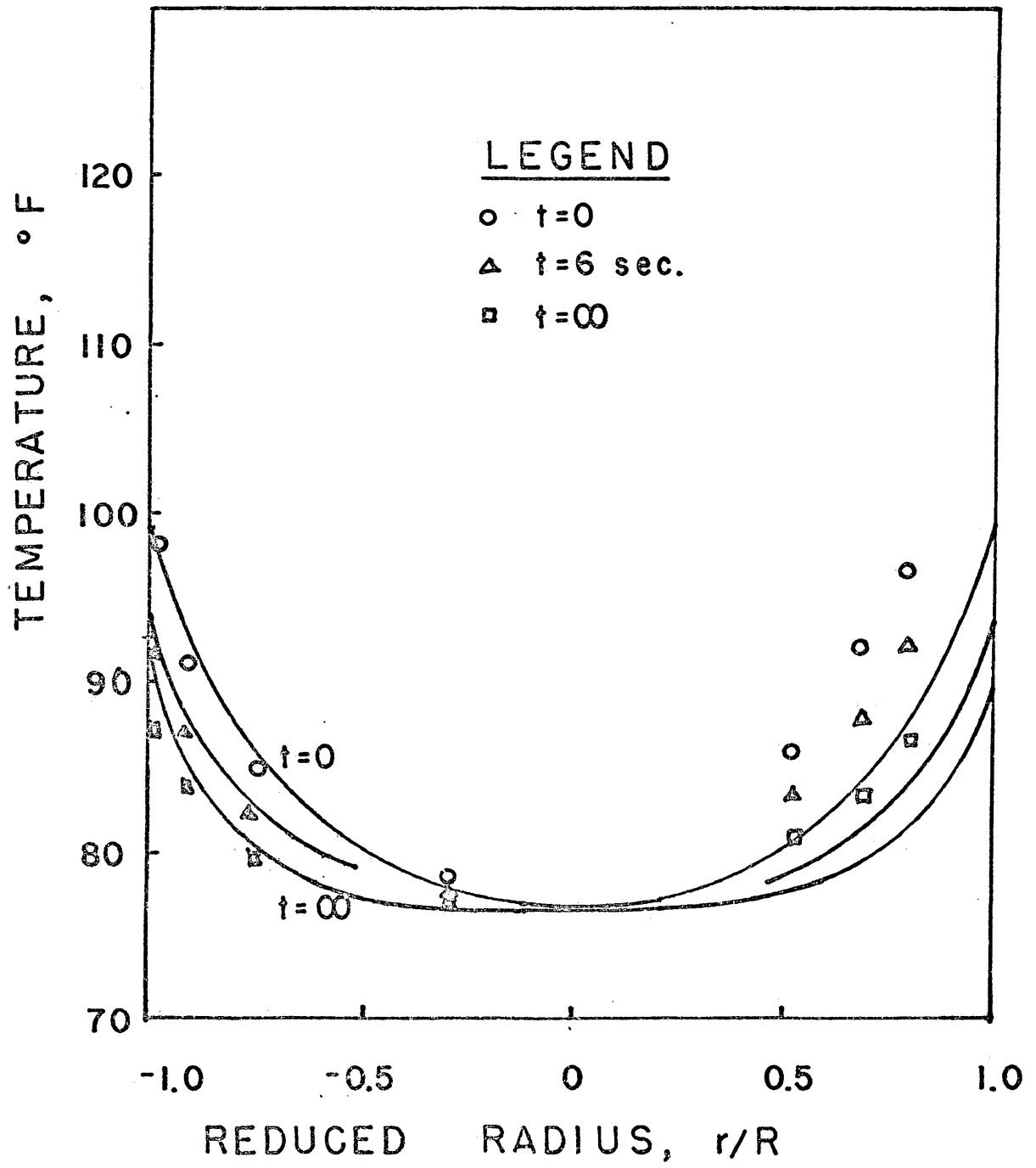
thermal conduction from surrounding fluid and this error can be neglected. For small heat flux the measuring error near the wall from which the thermocouple protrudes is much less than for large heat flux because the conduction driving force is smaller. A complete unsteady-state radial temperature profile has been presented in Fig. 13 for a low heat flux case. Even with a low heat flux the effect of the thermal conduction can be seen to make fluid temperature appear to be hotter close to the near wall than the far wall.

In laminar-flow heat transfer, the ratio L/D has been found by many engineers to be an important variable, where L is the length and D is the diameter of a heat exchanger. The heat transfer coefficient in laminar flow is dependent on this ratio. With constant physical properties, a smaller ratio of L/D gives a larger heat-transfer coefficient than a larger ratio of L/D . Sieder and Tate⁽¹⁷⁾ found the significant range of this L/D ratio to be from 60 to 240. In this experimental study one value of L/D equal to 102 was used.

Interesting phenomena were found in the transition range. The maximum N_{Re} in this experiment was 3875 for Run 9. In Run 9 the flow-rate change was made from laminar region ($N_{Re} = 1500$) to transition region ($N_{Re} = 3875$). As shown in Fig. 9, the transient temperature response at the central region of the tube showed an odd characteristic.

Figure 13. Experimental and theoretical fluid temperature vs radial position for Run 7^a with time as a parameter.

^aSee Table 2 for conditions of Run 7



When the step decrease in flow rate was made, the fluid temperature dropped instead of rising, and smoothly dropped to a certain temperature level. The temperature then rose to a new final steady-state temperature which was higher than the initial steady-state temperature. When the step decrease in flow rate was made, the temperature rose drastically in a short time and then settled to a new final steady-state temperature. This phenomenon may be explained as follows. When a step increase in flow rate is made, a fluid element in the central region of the tube obtains a drastic acceleration. Warmer fluid elements adjacent to the fluid in the center of the tube pick up momentum due to the natural convection and turbulence and look for a path in which to travel faster. Upon the onset of the step increase in flow rate, these fluid elements adjacent to the center contact neighboring fluid elements that travel very fast. Thus, fluid elements find a faster path and take it. The thermocouple at the exchanger outlet responds to this warm fluid and accordingly indicates higher temperature than the initial steady-state temperature. Therefore, an unstable hydrodynamic situation is created momentarily. When the new cool fluid comes from the inlet of the heat exchanger, it pushes out the warm fluid elements, and a new hydrodynamic stability is obtained. Similar reasoning applies to the

step decrease in flow rate. In the transition region it is felt that hydrodynamics play a highly important role in the transient temperature response.

As expected, Fig. 14 shows that before a time of L/u elapses, there is no dynamic temperature response to step changes in inlet temperature for all radial positions. Since an average velocity of fluid was used in this model, the theoretical dynamic temperature response of all radial position occurs at the same time of L/u . Actual dynamic temperature response at different radial positions would not occur at the same time because the fluid velocity, u , would be different for different radial positions. When a step change in inlet temperature is applied, a fluid temperature change at the outlet of the heat exchanger does not occur until the time L/u elapses. At time L/u after the step change in inlet temperature is made, the upset is observed at the exchanger outlet. Thus, in the theoretical model presented, the dynamic temperature response to a step change in inlet temperature occurs at time L/u , regardless of radial positions because of the average fluid-velocity assumption. It is expected that this would cause poor agreement between theoretical and experimental data at radial positions near the wall or center of a tube.

Figure 14. Theoretical fluid temperature response to transient inlet temperature changes between 70°F and 105°F with uniform wall temperature ^b

^bSee Table 3 for conditions of theoretical data

Inlet temperature decrease

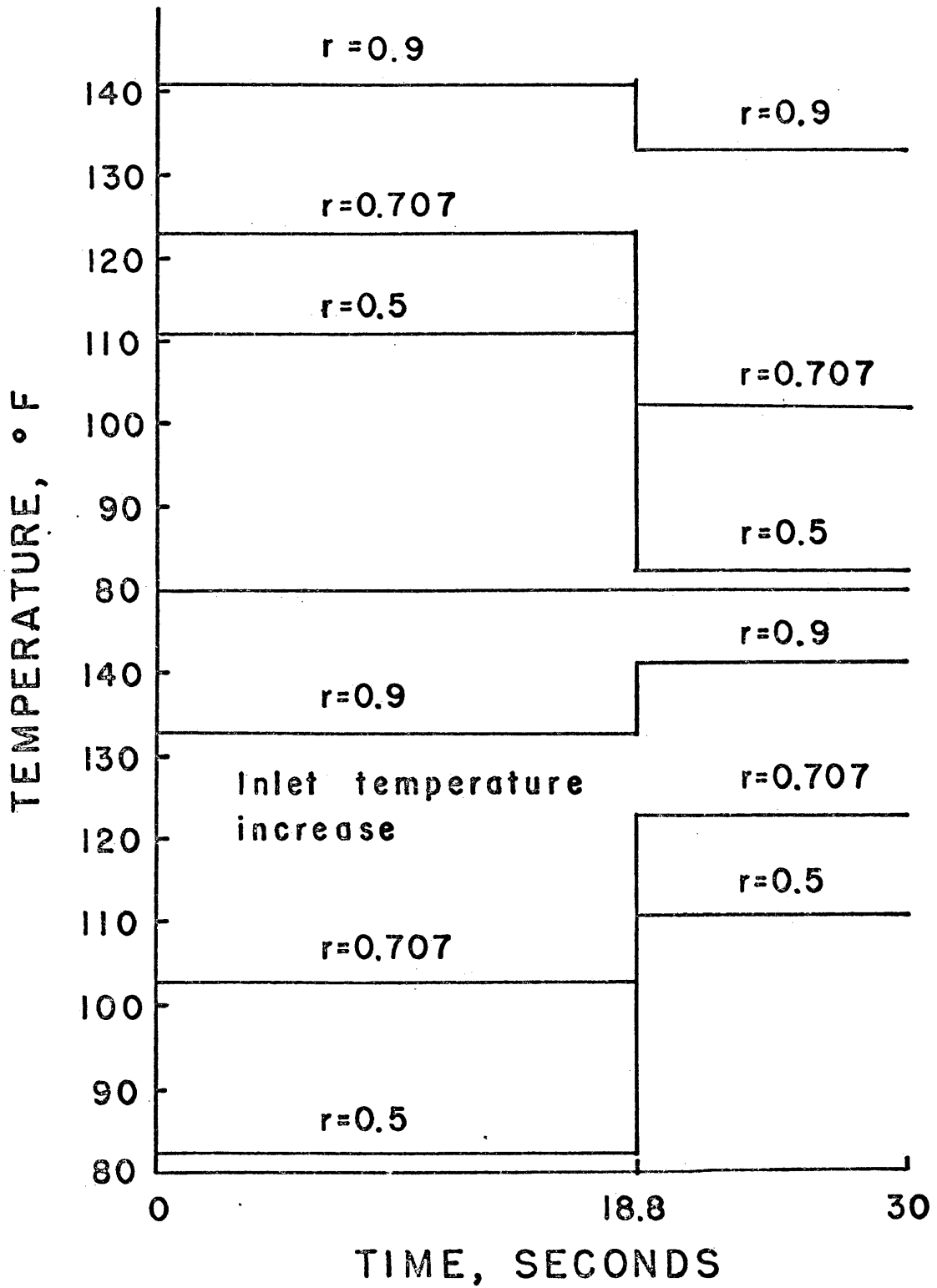


Figure 15 shows the theoretical dynamic fluid temperature response to step changes in flow rate with a uniform wall temperature. As expected these data are very similar to the data in Figs. 3 through 12 for flow upsets with uniform wall flux.

Figure 15. Theoretical fluid temperature response to transient flow changes between 0.269 ft/sec and 0.685 ft/sec with uniform wall temperature ^b

^bSee Table 4 for conditions of theoretical data

Flow rate decrease

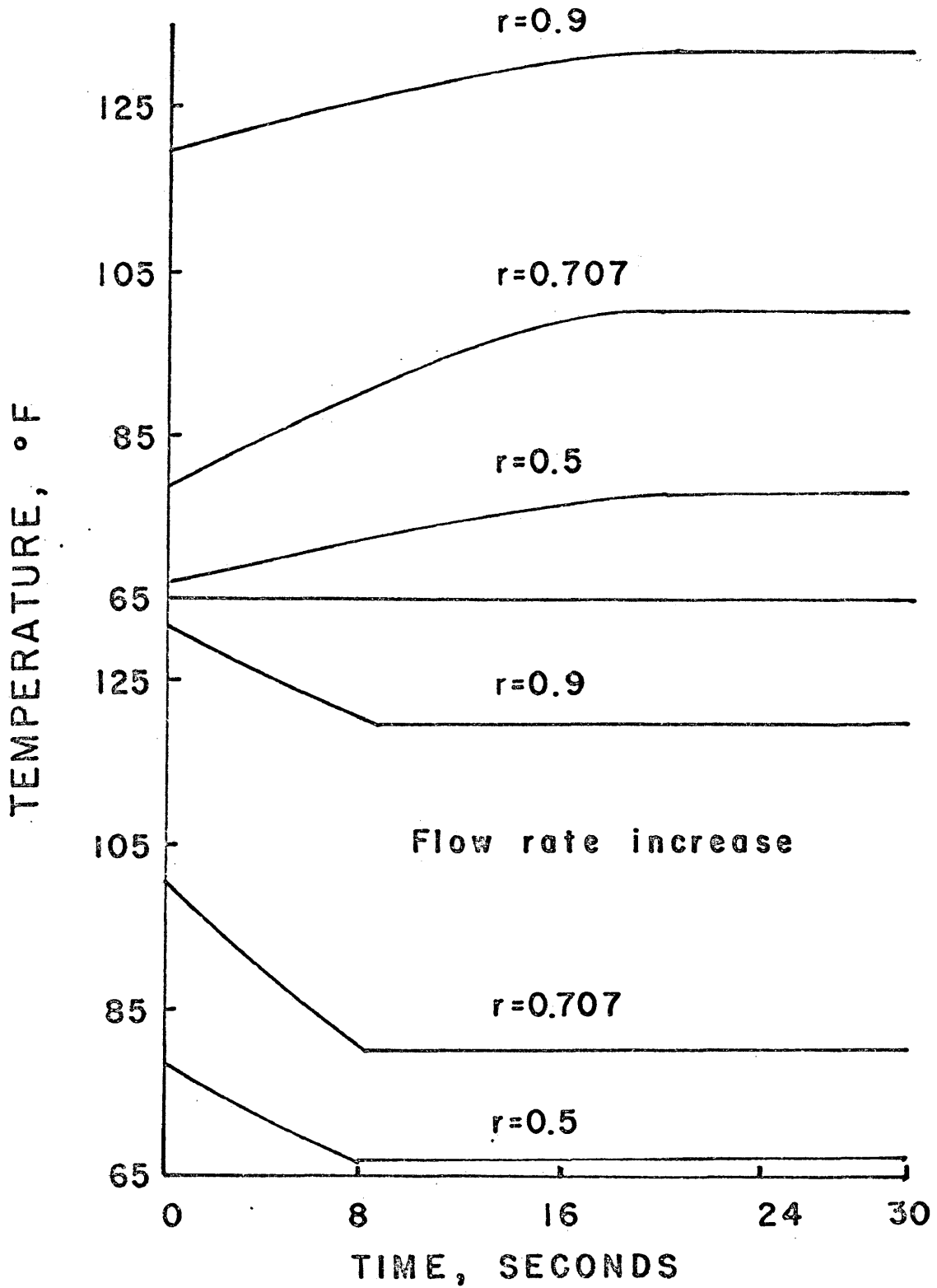


Figure 16. Qualitative change in velocity
profile by natural convection
proposed by Oliver

LEGEND^a

A Near inlet

B Further up tube

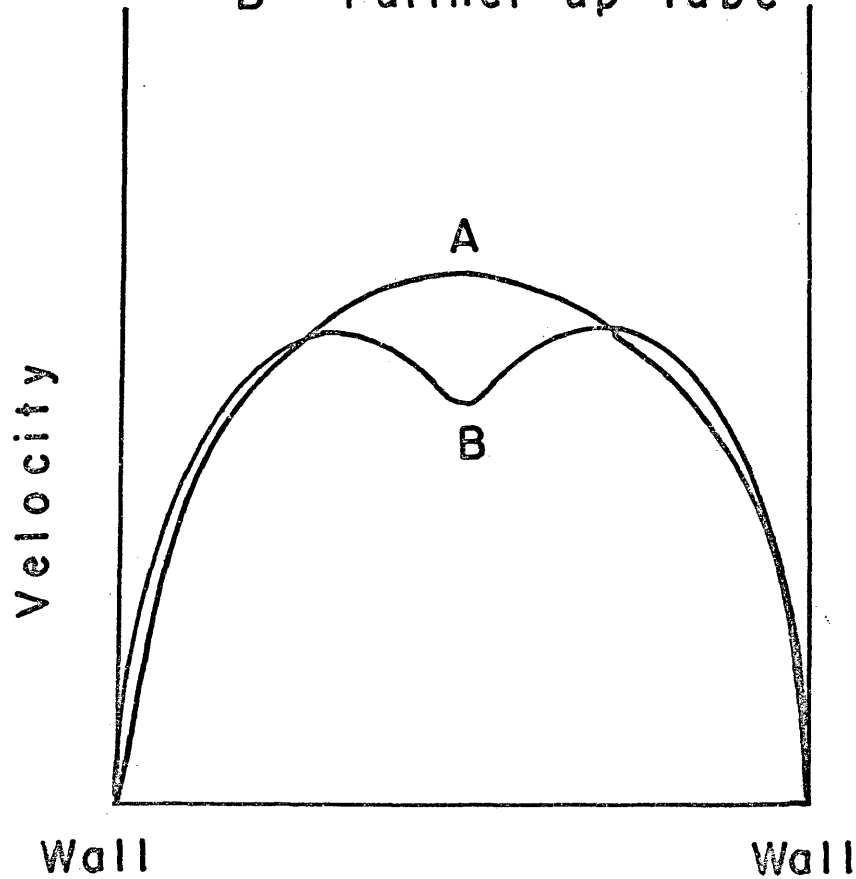


Fig.16 Change in velocity profile
by natural convection
(upward vertical flow and
heated wall)

^a Proposed by Oliver^b

^b See LITERATURE CITED 13

CONCLUSIONS

1. The combination of the Hankel transform technique and the method of characteristics is a powerful tool in solving a parabolic partial differential equation such as equation (1) solved in this dissertation. This method provided a model that gave reasonably good agreement with experimental data over the range of conditions investigated in this study.
2. There are two time domains in the dynamic response plane for a flow-forced heat exchanger. The characteristic line is $t = x/a$, which is the same as saying that the characteristic time equals the heat exchanger length divided by fluid velocity. Therefore, definite differences exist in the speed of response for increases and decreases in flow over the same flow range. Differences also exist at different radial positions because the exchanger length is always constant, but fluid velocity varies from radius to radius in laminar flow.

3. Experimental speed of response for step changes in flow rate is faster at the center and slower at the wall than the theoretical prediction due to the average velocity assumption used in the theoretical model. The speed of response of experimental and theoretical data agrees very well at the reduced radii approximately from 0.7 to 0.8. Agreement between theoretical and experimental data is not so good near the wall or the center of the tube because near the wall fluid travels much slower than average fluid velocity used in the model and near the center of the tube fluid travels faster than average velocity. Unless a precise velocity profile is known in a tube, it is impossible to know at what radial position the average velocity occurs. For non-isothermal flow it is very difficult to predict a reasonably accurate velocity profile, so use of the average velocity seems to be justified as pointed out by others⁽⁸⁾⁽¹²⁾.
4. The magnitude of flow-rate upset has a significant effect on the agreement between experimental and theoretical transient temperature response. As the magnitude of the flow-rate upset increases, the agreement between theoretical and experimental data becomes poor. It is proposed that this lack of agreement may be due to one or more of the following factors for large step changes

in flow rate: (1) a uniform wall heat-flux may not be sustained during the period of unsteady state due to the change of the heat transfer coefficient, (2) the nonlinearities in the physical system due to the change of physical properties of liquids become more prominent, and (3) fluid elements may have a turbulent mixing.

5. The ratio of N_{Gr}/N_{Re}^2 is very significant for determining the range of experimental conditions that give good experimental laminar-flow dynamic response data. With constant physical properties of the heat-exchanger liquid and a fixed length of the heat exchanger, the pertinent variable which determines the ratio is $\Delta T/u^2$. Thus, there are two variables, the inlet and outlet temperature difference and fluid velocity which can be manipulated to keep the ratio N_{Gr}/N_{Re}^2 as small as possible. Under the conditions of the present experimental study, the contribution of natural convection seemed to be significant when N_{Gr}/N_{Re}^2 was higher than 10, because random temperature response was obtained in this range.
6. In the transition region, the present model predicted the dynamic temperature response fairly well near the wall and poorly at the center of the tube. It is believed that a hydrodynamic instability occurs in the central region of the tube in the transition region,

and this instability causes poor agreement between theoretical and experimental data. It is believed that this hydrodynamic instability is caused by a combination of natural convection and turbulence due to the change in liquid density and fluid velocity.

7. Due to the average fluid velocity assumption made in this study, the theoretical dynamic temperature response to a step change in inlet temperature occurs at the same time L/u , regardless of the radial positions. Actual dynamic temperature response to a step change in inlet temperature would occur at different times for different radial positions since fluid velocity varies with radius in laminar flow. Since the model does not account for this variation, agreement between theoretical and experimental data would be expected to be poor near the wall or the center of the tube.
8. Theoretically, the dynamic temperature response to step changes in flow rate with a uniform wall temperature and with a uniform wall heat-flux is similar. Since reasonably good agreement was obtained between theory and experiment for uniform wall heat-flux, similar agreement should be obtained for the case of uniform wall temperature.

LITERATURE CITED

1. Sparrow, E. M., and Siegel, R., Unsteady state turbulent heat transfer in tubes: Jour. Heat Transfer, v. 82, p. 171, (1960).
2. Skegel, R., and Sparrow, E. M., Transient heat transfer for laminar forced convection in the thermal entrance region of flat ducts: Jour. Heat Transfer, v. 81, p. 29, (1959).
3. Siegel, R., and Perlmutter, M., Laminar heat transfer in a channel with unsteady flow and wall heating varying with position and time: Jour. Heat Transfer, v. 85, p. 358, (1963).
4. Siegel, R., Heat transfer for laminar flow in ducts with arbitrary time variation in wall temperature: Journ. Applied Mechanics, v. 27, p. 241, (1960).

5. Chu, S. C., and Bankoff, S. G., Unsteady heat transfer to slug flows; Effect of axial conduction: Am. Inst. Chem. Eng. Journ., v. 11, p. 607, (1965).
6. Zeiberg, S. L., and Muller, W. K., Transient laminar combined free and forced convection in a duct: Jour. Heat Transfer, v. 84, p. 141, (1962).
7. McAdams, W. H., Heat transmission: New York, McGraw Hill, p. 229, (1954).
8. Kirkbride, C. G., and McCabe, W. L., Heat transfer to liquids in viscous flow: Ind. Eng. Chem., v. 23, p. 625, (1931).
9. Bird, R. B., Stewart, W. E., and Lightfoot, E. N., Transport phenomena: New York, John Wiley and Sons, (1960).
10. International Critical Tables: New York, McGraw-Hill, (1928).
11. Sneddon, I. N., Elements of partial differential equation: New York, McGraw-Hill, (1957).
12. Boelter, L. M. K., Am. Inst. Chem. Eng. Trans., v. 39, p. 557, (1943).
13. Oliver, D. R., The effect of natural convection on viscous-flow heat transfer in horizontal tubes: Chem. Eng. Sci., v. 17, p. 335, (1962).

14. Acrivos, A., Combined laminar free- and forced-convection heat transfer in external flows: Am. Inst. Chem. Eng. Journ., v. 4, p. 285, (1958).
15. Kreith, F., Principles of heat transfer: Scranton, Pennsylvania, International Textbook Company, (1966).
16. Sparrow, E. M., and Gregg, J. L., Buoyancy effects in forced-convection flow and heat transfer: Jour. Applied Mechanics, v. 26, p. 133, (1959).
17. Sieder, E. N., and Tate, G. E., Heat transfer and pressure drop of liquids in tubes: Ind. Eng. Chem., v. 28, p. 1429, (1936).

NOMENCLATURE

a	u'/u_s
A	amplitude of sinusoidal disturbance
b	T_i/T_{ws}
c	T_w/T_{ws}
C_p	heat capacity, Btu/lb ^o F
D	heat exchanger diameter, ft
h	$\frac{\partial T}{\partial r^*} / \frac{\partial T_s}{\partial r^*} \Big _{r^* = R}$
k	thermal conductivity, Btu/ft hr ^o F
L	heat exchanger length, ft
n	integer
N_{Gr}	Grashof number, $\rho^2 g \gamma (T_{La} - T_i) L^3 / \mu^2$
N_{Pr}	Prandtle number, $C_p \mu / k$
N_{Re}	Reynolds number, $Du\rho/\mu$, or $Lu\rho/\mu$ for the ratio N_{Gr}/N_{Re}^2
q	heat flux, Btu/hr ft ²
r	reduced radius, r^*/R
r^*	radial coordinate, ft
R	heat exchanger radius, ft

S	heat transfer area, ft^2
t	reduced time, $4u_s t^* / DN_{\text{Res}} N_{\text{Pr}}$
t*	time, sec
T	temperature, $^{\circ}\text{F}$
u	fluid velocity (average), ft/sec
U	unit step function
W	liquid flow rate, lb/hr
w	frequency, rad/sec
x	reduced axial coordinate, $4x^* / DN_{\text{Res}} N_{\text{Pr}}$
x*	axial coordinate, ft
α	roots of bessel function $J_0(\alpha_n) = 0$
β	roots of the bessel function $J_1(\beta_n) = 0$
Δ	difference operator
Σ	summation
θ	reduced temperature
τ	dummy variable of t
ρ	density, lb/ft^3
γ	volumetric expansion coefficient

Subscript

a	average
i	refers to the inlet of the heat exchanger
L	refers to the axial distance $x^* = L$

s steady state value

w refers to the wall of the heat exchanger

Superscript

' deviation from initial steady state value

~~-----~~ Hankel transformed variable with respect to radial coordinate

APPENDIX A

Table 2. Initial and final state data for
ten experimental runs

Run 1. (59% glycerine 41% water)

$$T_i = 84^\circ\text{F} \quad q = 1900 \text{ Btu/ft}^2\text{hr}$$

<u>Reduced radius (r=r*/R)</u>	<u>Temperature (°F)</u>	
	<u>0.273 ft/sec</u>	<u>0.467 ft/sec</u>
1.0	135.8	116.6
0.91	115.4	102.2
0.79	104	96

Run 2. (59% glycerine 41% water)

$$T_i = 70^\circ\text{F} \quad q = 817 \text{ Btu/ft}^2\text{hr}$$

<u>Reduced radius (r=r*/R)</u>	<u>Temperature (°F)</u>	
	<u>0.188 ft/sec</u>	<u>0.309 ft/sec</u>
1.0	95.6	88.4
0.86	86	80
0.75	82.4	76
0.41	75.2	71.6

Table 2 (continued)

Run 3. (59% glycerine 41% water)

$$T_i = 63^\circ\text{F} \quad q = 817 \text{ Btu/ft}^2\text{hr}$$

<u>Reduced radius (r=r*/R)</u>	<u>Temperature ($^\circ\text{F}$)</u>	
	<u>0.188 ft/sec</u>	<u>0.418 ft/sec</u>
1.0	89	79.4
0.87	81	74
0.72	77.6	68.5
0.28	66.2	64.5

Run 4. (59% glycerine 41% water)

$$T_i = 67^\circ\text{F} \quad q = 1115 \text{ Btu/ft}^2\text{hr}$$

<u>Reduced radius (r=r*/R)</u>	<u>Temperature ($^\circ\text{F}$)</u>	
	<u>0.228 ft/sec</u>	<u>0.448 ft/sec</u>
1.0	99.2	84.5
0.85	89.6	77.6
0.62	77.6	68

Table 2 (continued)

Run 5. (59% glycerine 41% water)

$$T_i = 70^\circ\text{F} \quad q = 1115 \text{ Btu/ft}^2\text{hr}$$

<u>Reduced radius (r=r*/R)</u>	<u>Temperature (°F)</u>	
	<u>0.228 ft/sec</u>	<u>0.337 ft/sec</u>
1.0	107.6	96.8
0.88	96.8	87.2
0.78	83.6	75.2

Run 6. (59% glycerine 41% water)

$$T_i = 67^\circ\text{F} \quad q = 1115 \text{ Btu/ft}^2\text{hr}$$

<u>Reduced radius (r=r*/R)</u>	<u>Temperature (°F)</u>	
	<u>0.289 ft/sec</u>	<u>0.438 ft/sec</u>
1.0	93.2	84.8
0.85	81.8	75.6
0.76	77	71

Table 2 (continued)

Run 7. (43% glycerine 57% water)

$$T_i = 77^\circ\text{F} \quad q = 817 \text{ Btu/ft}^2\text{hr}$$

<u>Reduced radius (r=r*/R)</u>	<u>Temperature (°F)</u>	
	<u>0.269 ft/sec</u>	<u>0.568 ft/sec</u>
1.0	97.8	87.6
0.86	91.2	84
0.78	86.4	81

Run 8. (43% glycerine 57% water)

$$T_i = 77^\circ\text{F} \quad q = 817 \text{ Btu/ft}^2\text{hr}$$

<u>Reduced radius (r=r*/R)</u>	<u>Temperature (°F)</u>	
	<u>0.269 ft/sec</u>	<u>0.371 ft/sec</u>
1.0	97	93
0.90	93.6	88.8
0.81	88	84.8

Table 2. (continued)

Run 9. (0% glycerine 100% water)

$$T_i = 66^\circ\text{F} \quad q = 1115 \text{ Btu/ft}^2\text{hr}$$

<u>Reduced radius (r=r*/R)</u>	<u>Temperature ($^\circ\text{F}$)</u>	
	<u>0.269 ft/sec</u>	<u>0.685 ft/sec</u>
1.0	95.8	76.8
0.94	87.6	71.4
0.47	70.4	71.4

Run 10. (0% glycerine 100% water)

$$T_i = 66^\circ\text{F} \quad q = 1115 \text{ Btu/ft}^2\text{hr}$$

<u>Reduced radius (r=r*/R)</u>	<u>Temperature ($^\circ\text{F}$)</u>	
	<u>0.69 ft/sec</u>	<u>0.355 ft/sec</u>
1.0	89.8	84.5
0.88	80	74.4
0.27	66	67

APPENDIX B

Table 3. Initial and final steady-state theoretical data for a step change in inlet temperature with uniform wall temperature

(0% glycerine 100% water)

$u = 0.269$ ft/sec ($N_{Re} = 1528$)

$T_w = 150^\circ\text{F}$

<u>Reduced radius ($r=r^*/R$)</u>	<u>Temperature ($^\circ\text{F}$)</u>	
	<u>70°F</u>	<u>105°F</u>
0.9	133	141
0.707	103	123
0.50	82	111

APPENDIX C

Table 4. Initial and final steady-state theoretical data for a step change in flow rate with uniform wall temperature

(0% glycerine 100% water)

$$T_w = 150^{\circ}\text{F}$$

$$T_i = 66^{\circ}\text{F}$$

<u>Reduced radius (r=r*/R)</u>	<u>Temperature ($^{\circ}\text{F}$)</u>	
	<u>0.269 ft/sec</u>	<u>0.682 ft/sec</u>
0.9	131	120
0.707	100	78.7
0.50	79	66

APPENDIX D

Table 5. Physical properties of glycerine-water mixture at 30°C

	<u>Volume percent of liquid</u>		
	59% glycerine 41% water	43% glycerine 57% water	0% glycerine 100% water
Density (gr/cc)	1.148	1.103	0.995
Viscosity (centipoise)	12.25	3.7	0.80
Thermal conductivity (Btu/hr ft °F)	0.207	0.246	0.35
Specific heat capacity (Btu/lb °F)	0.717	0.814	0.998

APPENDIX E

Table 6. Duplicate experimental runs at the same conditions as the experimental runs presented in the dissertation.

<u>Run 1^a</u>	<u>Temperature (°F)</u>					
	<u>Flow decrease</u>		<u>Flow increase</u>			
	r=1.0	r=0.91	r=0.79	r=1.0	r=0.91	r=0.79
0	120	102.8	95	135.8	114.2	103
6	124.8	109	100	125	106	97.2
12	127.8	113	102.5	120	103	96
18	130	114	103.6	119	102.8	96
24	130.6	114.5	103.6	118.8	102.5	96
30	130.6	114.9	103.6	117.8	102.4	96

^aSee Table 2 for all conditions of runs.

Table 6 (continued)

Run 2

<u>Time (sec)</u>	<u>Temperature (°F)</u>					
	<u>Flow increase</u>			<u>Flow decrease</u>		
	r=1.0	r=0.86	r=0.75	r=1.0	r=0.86	r=0.75
0	95.5	86	82	88.5	80	76
6	94	82.5	80	91.2	81.2	78
12	91.2	80.5	78.5	93.8	83.5	79.5
18	90.8	80	77.5	94	84.5	80
24	90.5	80	77	95	85.5	80.5
30	90.5	80	76.8	95.5	86.2	81.2

Run 3

<u>Time (sec)</u>	<u>Temperature (°F)</u>					
	<u>Flow increase</u>			<u>Flow decrease</u>		
	r=1.0	r=0.87	r=0.72	r=1.0	r=0.87	r=0.72
0	89	81	76	80	74	69
6	84.5	77	72	81.2	75	73
12	82	75	70	83.5	76.5	74
18	81.9	75	69.5	84.5	78.5	74.5
24	81.8	75	69.5	86	79	76
30	81.8	75	69.3	87	79	77

Table 6 (continued)

Run 4

<u>Time (sec)</u>	<u>Temperature (°F)</u>					
	<u>Flow increase</u>				<u>Flow decrease</u>	
	r=1.0	r=0.85	r=0.62	r=1.0	r=0.85	r=0.62
0	98	89	77	85.5	77.5	68
6	91	82	69	89	81.5	70.5
12	87.5	79	68	91.5	83.5	73
18	86.5	78.5	68	94	85.5	75
24	86	78.2	68	95	86.2	76
30	85.5	78.2	68	97	86.6	77

Run 5

<u>Time (sec)</u>	<u>Temperature (°F)</u>					
	<u>Flow increase</u>				<u>Flow decrease</u>	
	r=1.0	r=0.88	r=0.78	r=1.0	r=0.88	r=0.78
0	104	95	81	96	85	76
6	101	90.5	78	99	88	79
12	98.5	89	77	101	90.5	80.5
18	98	87	76	102	92	82
24	97	87	76	103	92.5	82
30	97	87	76	103.5	93	82

Table 6 (continued)

Run 6

<u>Time (sec)</u>	<u>Temperature (°F)</u>					
	<u>Flow increase</u>				<u>Flow decrease</u>	
	r=1.0	r=0.85	r=0.76	r=1.0	r=0.85	r=0.76
0	95	81	74	86	75	70.5
6	89	78	73	90	78.5	74
12	88	75.8	71	91	79.5	75.2
18	87.8	75.8	70.8	91.5	79	75.8
24	87.5	75.8	70.5	92.5	80	76
30	87.5	75.8	70.5	93	80	76

Run 7

<u>Time (sec)</u>	<u>Temperature (°F)</u>					
	<u>Flow increase</u>				<u>Flow decrease</u>	
	r=1.0	r=0.86	r=0.78	r=1.0	r=0.86	r=0.78
0	97.8	91.2	86	88.5	84	80.5
6	91.5	87	82	91.5	87	82.5
12	90.5	85.5	81.2	94	88	84
18	90	85	80.5	95	89.5	85
24	89.5	84.5	80.5	95.5	90	85.5
30	89.5	84.5	80.5	96	90.2	85.5

Table 6 (continued)

Run 8

<u>Time (sec)</u>	<u>Temperature (°F)</u>					
	<u>Flow increase</u>		<u>Flow decrease</u>			
	r=1.0	r=0.9	r=0.81	r=1.0	r=0.9	r=0.81
0	98.2	92.5	87.8	93	89.4	84.6
6	96	91.2	86.3	94.5	90.6	85.8
12	94.5	90	85.8	95.5	91.4	86.9
18	94	89.5	85.5	96.2	92.2	87.2
24	93.5	89.5	85.5	96.5	92.5	87.3
30	93.5	89.5	85.5	96.5	92.5	87.3

Run 9

<u>Time (sec)</u>	<u>Temperature (°F)</u>					
	<u>Flow increase</u>		<u>Flow decrease</u>			
	r=1.0	r=0.94	r=0.47	r=1.0	r=0.94	r=0.47
0	93.5	86.5	70	77.7	72	70
6	87	80.5	67	80	75.5	69
12	83.5	77	71.5	83	77.5	67
18	80	75	70	85.5	79	67
24	78.5	68	70	86.2	81	68
30	78.2	68	70	88.2	83.5	69

Table 6 (continued)

Run 10

<u>Time (sec)</u>	<u>Temperature (°F)</u>					
	<u>Flow increase</u>				<u>Flow decrease</u>	
	r=1.0	r=0.88	r=0.27	r=1.0	r=0.88	r=0.27
0	89.8	80	66	84.4	75.5	66
6	86.5	77	67.5	86.5	77.2	67.2
12	85.2	76	66.6	87.5	78.4	68
18	84.4	76	66.3	88.3	78.6	68.4
24	84.4	76	66.3	89	79.2	68.4
30	84.4	76	66.3	89.2	79.2	68.6